Article

Cell Reports

Guanylate-Binding Proteins 2 and 5 Exert Broad Antiviral Activity by Inhibiting Furin-Mediated Processing of Viral Envelope Proteins

Graphical Abstract

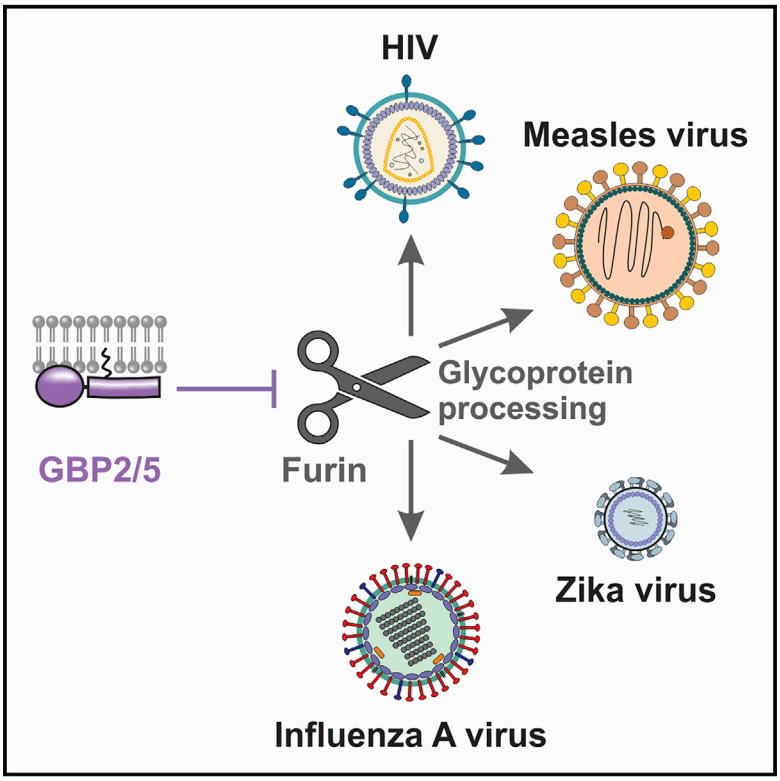

Authors

Elisabeth Braun, Dominik Hotter, Lennart Koepke, ..., Oliver T. Fackler, Frank Kirchhoff, Daniel Sauter

Correspondence

daniel.sauter@uni-ulm.de

In Brief

The cellular protease furin processes numerous substrates, including the envelope proteins of many viral pathogens. Here, Braun et al. show that guanylate-binding proteins 2 and 5 are interferon-inducible restriction factors that reduce virion infectivity by inhibiting furin activity and consequently maturation of viral envelope glycoproteins.

Highlights

- Guanylate-binding proteins 2 and 5 inhibit the host protease furin
- GBP2/5 suppress furin-mediated priming of diverse viral envelope glycoproteins
- GBP2/5 reduce replication of HIV-1, Zika, measles, and influenza A viruses
- GBP2/5 also reduce furin-mediated processing of cellular proteins

Braun et al., 2019, Cell Reports 27, 2092–2104
May 14, 2019
https://doi.org/10.1016/j.celrep.2019.04.063

CellPress

OPEN ACCESS
CellPress

Cell Reports
Article

Guanylate-Binding Proteins 2 and 5 Exert Broad Antiviral Activity by Inhibiting Furin-Mediated Processing of Viral Envelope Proteins

Elisabeth Braun,[1,11] Dominik Hotter,[1,11] Lennart Koepke,[1] Fabian Zech,[1] Rüdiger Groß,[1] Konstantin M.J. Sparrer,[1] Janis A. Müller,[1] Christian K. Pfaller,[2] Elena Heusinger,[1] Rebecka Wombacher,[3] Kathrin Sutter,[4] Ulf Dittmer,[4] Michael Winkler,[5] Graham Simmons,[6] Martin R. Jakobsen,[7] Karl-Klaus Conzelmann,[8] Stefan Pöhlmann,[5,9] Jan Münch,[1] Oliver T. Fackler,[3,10] Frank Kirchhoff,[1] and Daniel Sauter[1,12,*]

[1]Institute of Molecular Virology, Ulm University Medical Center, Ulm 89081, Germany
[2]Paul-Ehrlich-Institute, Langen 63225, Germany
[3]Center for Integrative Infectious Disease Research, Integrative Virology, University Hospital Heidelberg, Heidelberg 69120, Germany
[4]Institute for Virology, University Clinics Essen, University of Duisburg-Essen, Essen 45147, Germany
[5]Infection Biology Unit, German Primate Center - Leibniz Institute for Primate Research, Göttingen 37077, Germany
[6]Blood Systems Research Institute, Department of Pathology and Laboratory Medicine, University of California, San Francisco, San Francisco, CA 94118, USA
[7]Department of Biomedicine, Aarhus University, Aarhus 8000, Denmark
[8]Max von Pettenkofer Institute Virology, Medical Faculty, and Gene Center, Ludwig-Maximilians-University Munich, Munich 81377, Germany
[9]Faculty of Biology and Psychology, University Göttingen, Göttingen 37073, Germany
[10]German Center for Infection Research (DZIF), Partner Site Heidelberg, Heidelberg 69120, Germany
[11]These authors contributed equally
[12]Lead Contact
*Correspondence: daniel.sauter@uni-ulm.de
https://doi.org/10.1016/j.celrep.2019.04.063

SUMMARY

Guanylate-binding protein (GBP) 5 is an interferon (IFN)-inducible cellular factor reducing HIV-1 infectivity by an incompletely understood mechanism. Here, we show that this activity is shared by GBP2, but not by other members of the human GBP family. GBP2/5 decrease the activity of the cellular proprotein convertase furin, which mediates conversion of the HIV-1 envelope protein (Env) precursor gp160 into mature gp120 and gp41. Because this process primes HIV-1 Env for membrane fusion, viral particles produced in the presence of GBP2/5 are poorly infectious due to increased incorporation of nonfunctional gp160. Furin activity is critical for the processing of envelope glycoproteins of many viral pathogens. Consistently, GBP2/5 also inhibit Zika, measles, and influenza A virus replication and decrease infectivity of viral particles carrying glycoproteins of Marburg and murine leukemia viruses. Collectively, our results show that GPB2/5 exert broad antiviral activity by suppressing the activity of the virus-dependency factor furin.

INTRODUCTION

Infection with HIV and other viral pathogens triggers the production of interferons (IFNs), which induce an antiviral cellular state by upregulating the expression of hundreds of IFN-stimulated genes (ISGs). The products of these genes exert numerous effector functions and may target essentially every step of the viral replication cycle. Among the earliest identified ISGs were guanylate-binding proteins (GBPs) (Cheng et al., 1983; Staeheli et al., 1984). It was their marked IFN-inducibility that helped to decipher the type I and II IFN signaling cascades (Decker et al., 1989; Lew et al., 1991). The human genome encodes seven members of this protein family (GBP1–7), all of which are assumed to act as GTPases hydrolyzing GTP to GDP and GMP (Vestal and Jeyaratnam, 2011). Together with Myxoma resistance proteins (MxA and MxB), immunity-related GTPases (IRGs), and very large inducible GTPases (VLIGs), GBPs form the superfamily of so-called IFN-inducible GTPases (Kim et al., 2012). Although numerous studies characterized the restriction of influenza A viruses and HIV by Mx proteins (reviewed in Haller et al., 2015), little is known about the antiviral activity of other members of this superfamily.

GBPs are probably the most enigmatic of all IFN-inducible GTPases. Initially described as cellular factors providing resistance against bacterial and protozoan pathogens (Vestal and Jeyaratnam, 2011), they were subsequently also shown to be important components of the immune defense against viruses. For example, GBP1 has been shown to restrict vesicular stomatitis virus (VSV), encephalomyocarditis virus (EMCV), and hepatitis C virus (HCV) by yet unknown mechanism(s) (Anderson et al., 1999; Itsui et al., 2006, 2009). Furthermore, a splice variant of human GBP3 (hGBP-3ΔC) suppresses influenza A virus replication by inhibiting the viral polymerase complex (Nordmann et al., 2012). In addition, genome-wide association studies suggest a potential role of porcine GBPs in resistance to porcine reproduction and respiratory syndrome virus (PRRSV) infection (Rowland et al., 2012). Finally, we have recently shown that GBP5 reduces HIV-1 infectivity by interfering with maturation and virion

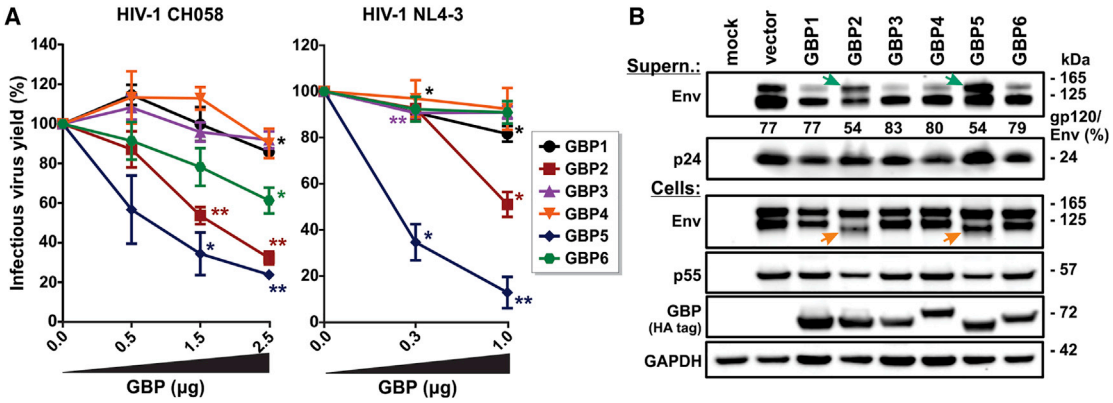

Figure 1. GBP2 and GBP5 Interfere with HIV-1 Env Maturation and Reduce Infectivity of HIV-1

(A) HEK293T cells were co-transfected with a proviral construct of HIV-1 CH058 (left panel) or NL4-3 (right panel) and increasing amounts of an expression plasmid for the indicated GBPs. Two days posttransfection, infectious virus yield was determined by infection of TZM-bl reporter cells. Mean values of three independent experiments ± SEM are shown. Asterisks indicate statistically significant differences compared with the control without GBP.

(B) Cells were transfected as described in (A) using HIV-1 CH058 and 1.5 μg GBP expression plasmid. Two days posttransfection, cells and supernatants were lysed for western blot analysis. Green and orange arrowheads indicate an altered virion incorporation of gp120/gp160 and a reduced apparent molecular weight of cellular gp120, respectively. Band intensities were quantified to calculate the ratio of gp120 to total Env.

See also Figure S1.

incorporation of the envelope glycoprotein (Env) (Hotter et al., 2017; Krapp et al., 2016). Our findings showed that GTPase activity is dispensable for the anti-HIV activity of GBP5 (Krapp et al., 2016). However, it remained unclear how this cellular factor decreases virion infectivity. Thus, the main objective of the present study was to elucidate the mechanism(s) underlying the antiretroviral activity of GBP5. Furthermore, we aimed to determine whether other GBP protein family members exert similar restriction activity and to define their breadth of antiviral activity. Comparing the antiviral activity of different GBP paralogs, we found that the ability of GBP5 to reduce HIV infectivity is shared by its paralog GBP2. In addition, we show that both factors exert broad antiviral activity as they suppress proteolytic processing of envelope glycoproteins from numerous viral pathogens by inhibiting the cellular protease furin. Thus, we here identify a mechanism of antiviral immunity that involves the inhibition of a crucial virus-dependency factor.

RESULTS

GBP2 and GBP5 Interfere with HIV-1 Env Maturation in Primary Target Cells

The human *GBP* locus comprises seven genes (*GBP1–7*) (Olszewski et al., 2006). To test their anti-HIV-1 activity, we amplified *GBP1–6* using cDNA from peripheral blood mononuclear cells (PBMCs). *GBP7* was not amplified because its expression is largely restricted to the liver (Human Protein Atlas available from https://www.proteinatlas.org; Uhlén et al., 2015). Titration experiments of GBP1–6 in transfected HEK293T cells, which do not express endogenous GBP1–7 (Uhlén et al., 2015), revealed that GBP2 shares the ability of GBP5 to inhibit infectious HIV-1 yield (Figure 1A). All remaining GBPs had no (GBP3/4) or only minor (GBP1/6) effects on infectious HIV-1 yield. GBP2 and GBP5 reduced the ratio of mature gp120 to total Env in HIV-1 virions (Figure 1B, green arrows), whereas other GBP proteins did not affect Env maturation. In agreement with a maturation defect, an Env product with reduced apparent molecular weight compared with regular gp120 accumulated in the cells (Figure 1B, orange arrows). This shift could previously be ascribed to reduced N-linked Env glycosylation (Krapp et al., 2016). Inhibition of infectious virus production and interference with Env maturation were abrogated upon mutation of the C-terminal isoprenylation motif (CaaX) in GBP2/5 (Figures S1A and S1B), suggesting that membrane anchoring is required for restriction. Notably, increased GBP expression did not affect cell viability in transient transfection assays (Figure S1C).

To monitor GBP2/5 expression in primary cells, we first validated the specificity of GBP2 and GBP5 antibodies using HEK293T cells transfected with hemagglutinin (HA)-tagged versions of GBP1–6 (Figure S2A). Western blot and/or flow cytometric analyses of primary human monocyte-derived macrophages (MDMs) and $CD4^+$ T cells demonstrated that both GBP2 and GBP5 are constitutively expressed but further upregulated upon HIV-1 infection (Figure S2B) and stimulation with IFNα2 and/or IFNγ (Figure 2A). Although IFNα2 is most commonly used in clinical trials, some of its paralogs, particularly IFNα14, suppress HIV-1 replication more efficiently (Abraham et al., 2016; Harper et al., 2015; Lavender et al., 2016). Notably, IFNα14 was also the most potent inducer of GBP5 among all 12 human IFNα subtypes (Figures 2B and S2C). Although activation via anti-CD3/CD28 beads is frequently used to render $CD4^+$ T cells permissive to HIV-1, it also increased GBP2/5 expression by ~2- to 5-fold (Figure 2A). However, this induction may be indirect because CD3/T cell receptor activation is known to trigger release of IFNγ, interleukin-2 (IL-2), and other cytokines (Girdlestone and Wing, 1996). Notably, endogenous GBP2/5 levels upon IFNγ stimulation of primary macrophages were similar to those of HEK293T cells transfected with low amounts of the respective expression plasmids (Figure S2D).

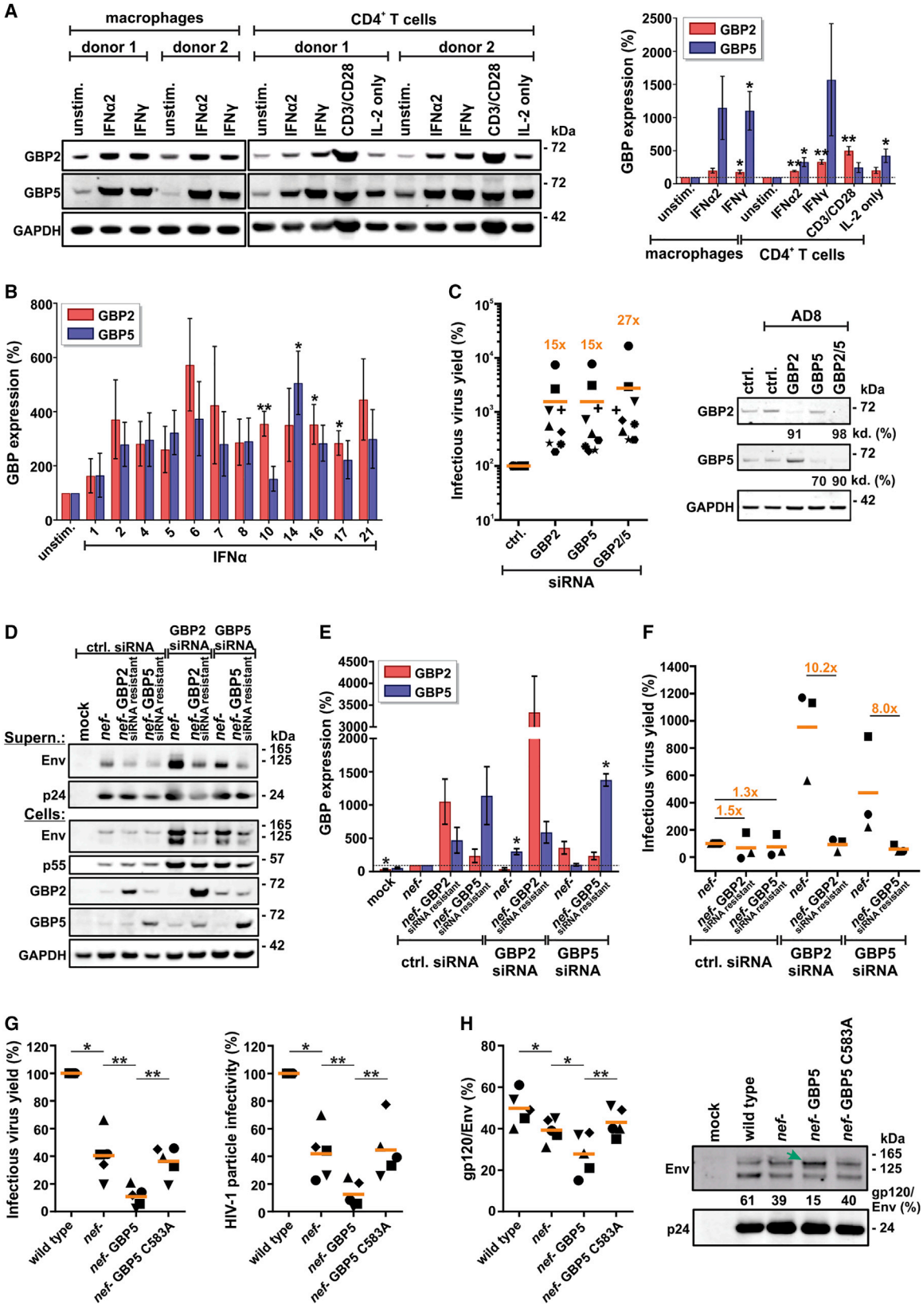

(legend on next page)

Individual knockdown of GBP2 and GBP5 in MDMs increased infectious virus yield ~15-fold, whereas a combined knockdown had additive effects resulting in ~27-fold higher infectious HIV-1 yield (Figure 2C, left panel; Figure S2E). In some donors, GBP5 levels increased upon GBP2 silencing (Figure 2C, right panel), indicating a potential compensatory feedback mechanism of both proteins. However, this increase was statistically not significant (Figure S2F). To restore GBP expression, we generated HIV-1 chimeras encoding GBP2 or GBP5. We selected the well-characterized NL4-3 clone (HIV-1 M subtype B) and replaced the accessory gene *nef* by siRNA-resistant forms of *GBP2* or *GBP5* (Figure S2G). A *nef*-defective construct served as control. Western blotting confirmed efficient rescue of GBP2/5 expression upon infection of siRNA-treated macrophages with GBP2/5-encoding viruses (Figures 2D and 2E). GBP2 and GBP5 re-expression affected the processing of Env, reduced the incorporation of mature gp120 into virions (Figure 2D), and decreased infectious virus production (Figures 2F and S2H). As expected, the inhibitory effects of GBP2/5 on infectious virus yield were more pronounced in GBP-knockout than in control siRNA-treated cells (Figure 2F).

To validate the inhibitory activity of GBPs in primary lymphoid cells, we performed experiments in human lymphoid aggregate cultures (HLACs) derived from tonsillar explants. Because efficient siRNA-mediated knockout has proved to be difficult in primary $CD4^+$ T cells, we infected them with chimeric viruses expressing GBP5 or the isoprenylation-deficient mutant (C583A) thereof (Figures S2I and S2J). As expected (Chowers et al., 1994), loss of Nef decreased total infectious virus yield and infectivity per viral particle (Figure 2G). Intriguingly, expression of wild-type (WT) GBP5, but not the isoprenylation-deficient mutant, further reduced infectivity by ~75% (Figure 2G). This effect was independent of infection rates (Figure S2K) but coincided with a decreased ratio of mature gp120 to total Env in the virions (Figure 2H, right panel, green arrow). Altogether, these results demonstrate that GBP2 and GBP5 are IFN-inducible restriction factors that reduce HIV-1 particle infectivity in primary macrophages and tonsillar lymphoid cells.

GBP2 and GBP5 Do Not Directly Target Env to Restrict HIV-1

To compare the subcellular localization of GBPs, we generated eGFP-GBP fusion proteins. Addition of an eGFP-tag did not affect the ability of GBP5 to interfere with infectious virus yield (Figure S3A) or Env processing (Figure S3B). In agreement with the presence of a C-terminal membrane anchor, GBP1, GBP2, and GBP5 localized to large intracellular vesicles and/or compartments that appeared more compact for GBP5 than for GBP1 and GBP2 (Figures 3A and S3C). Consistent with previous findings (Britzen-Laurent et al., 2010), GBP5-containing structures partially co-localized with the *trans*-Golgi marker TGN46 (Figures 3A and S3C, arrowheads), whereas no such co-localization was observed for GBP1 and GBP2. Surprisingly, GBP4 and GBP6 also accumulated in mostly TGN46-negative intracellular vesicle-like structures, although they do not harbor a C-terminal isoprenylation site (Figure S3C). In contrast, GBP3 and the isoprenylation-deficient mutants of GBP2 and GBP5 were diffusely distributed throughout the cytoplasm (Figures 3A and S3C).

HIV-1 Env is N-glycosylated and proteolytically processed on its route to the cell surface via the endoplasmic reticulum (ER), cytoplasmic vesicles, and the Golgi apparatus (Moulard and Decroly, 2000). We therefore examined whether GBP2/5 may target the accessible cytoplasmic tail of Env (Figure 3B, left panel) to interfere with its maturation and anterograde transport to sites of viral budding. Indeed, GBP2/5 expression reduced Env protein levels at the cell surface by 55% to 75% (Figure 3B, right panel; Figure S3D). However, deletion of the Env cytoplasmic domain (ΔCT) or exchange of its transmembrane

Figure 2. GBP2 and GBP5 Are IFN-Inducible Proteins that Reduce Virion Infectivity in Primary HIV-1 Target Cells

(A) Monocyte-derived macrophages were stimulated with IFNα2 or IFNγ. $CD4^+$ T cells were stimulated with IL-2 + IFNα2, IL-2 + IFNγ, IL-2 + anti-CD3/CD28 beads, or IL-2 alone. Three days poststimulation, cells were lysed for western blot analysis. GBP expression levels were quantified and normalized to the respective untreated control (unstim.). Exemplary blots showing GBP expression in cells from two different donors are shown on the left. Mean values ± SEM obtained from cells of five different donors are shown on the right. Asterisks indicate statistically significant differences compared with the untreated control (unstim.).

(B) $CD4^+$ T cells were stimulated with the indicated IFNα subtypes. Three days poststimulation, cells were lysed for western blot analysis. GBP expression levels were quantified and normalized to the respective untreated control (unstim.). Mean values ± SEM obtained from cells of four to five different donors are shown. Asterisks indicate statistically significant differences compared with the unstimulated control (unstim.).

(C) Monocyte-derived macrophages were transfected with the indicated siRNAs and infected with HIV-1 AD8. Six days postinfection, infectious virus yield was determined by infection of TZM-bl reporter cells (left panel). Numbers indicate n-fold increase. Knockdown efficiencies were determined by western blotting. One representative western blot and the respective knockdown efficiencies of GBP2/5 are shown in the right panel.

(D–F) Monocyte-derived macrophages were transfected with the indicated siRNAs and infected with VSV-G-pseudotyped HIV-1 NL4-3-expressing siRNA-resistant GBP2/5 instead of Nef or neither Nef nor GBP (*nef*−).

(D and E) GBP2/5 expression as well as Env protein levels were analyzed by western blotting 6 days after infection. One representative western blot is shown. Mean values ± SEM of the three donors analyzed in (D) are shown in (E). Asterisks indicate significant differences compared with the control (ctrl). siRNA samples infected with *nef*-deficient NL4-3 (100%).

(F) Infectious virus yield was determined by infection of TZM-bl reporter cells. Numbers indicate n-fold differences.

(G) Human lymphoid aggregate cultures (HLACs) were isolated from tonsillar explants and infected with HIV-1 NL4-3, expressing GBP5 or an isoprenylation-deficient mutant thereof instead of Nef, or the respective wild-type and *nef*-deficient controls. Three days postinfection, infectious virus yield (left panel) was determined by infection of TZM-bl reporter cells and normalized to the amount of p24 to calculate particle infectivity (right panel).

(H) Env protein levels in virions produced from HLACs described in (G) were analyzed by western blotting. One exemplary western blot is shown in the right panel. Band intensities were quantified to calculate the ratio of gp120 to total Env (left panel).

In (C) and (F)–(H), each data point represents one independent donor, and mean values are indicated by a horizontal line. In (G) and (H), asterisks indicate significant differences.

See also Figure S2.

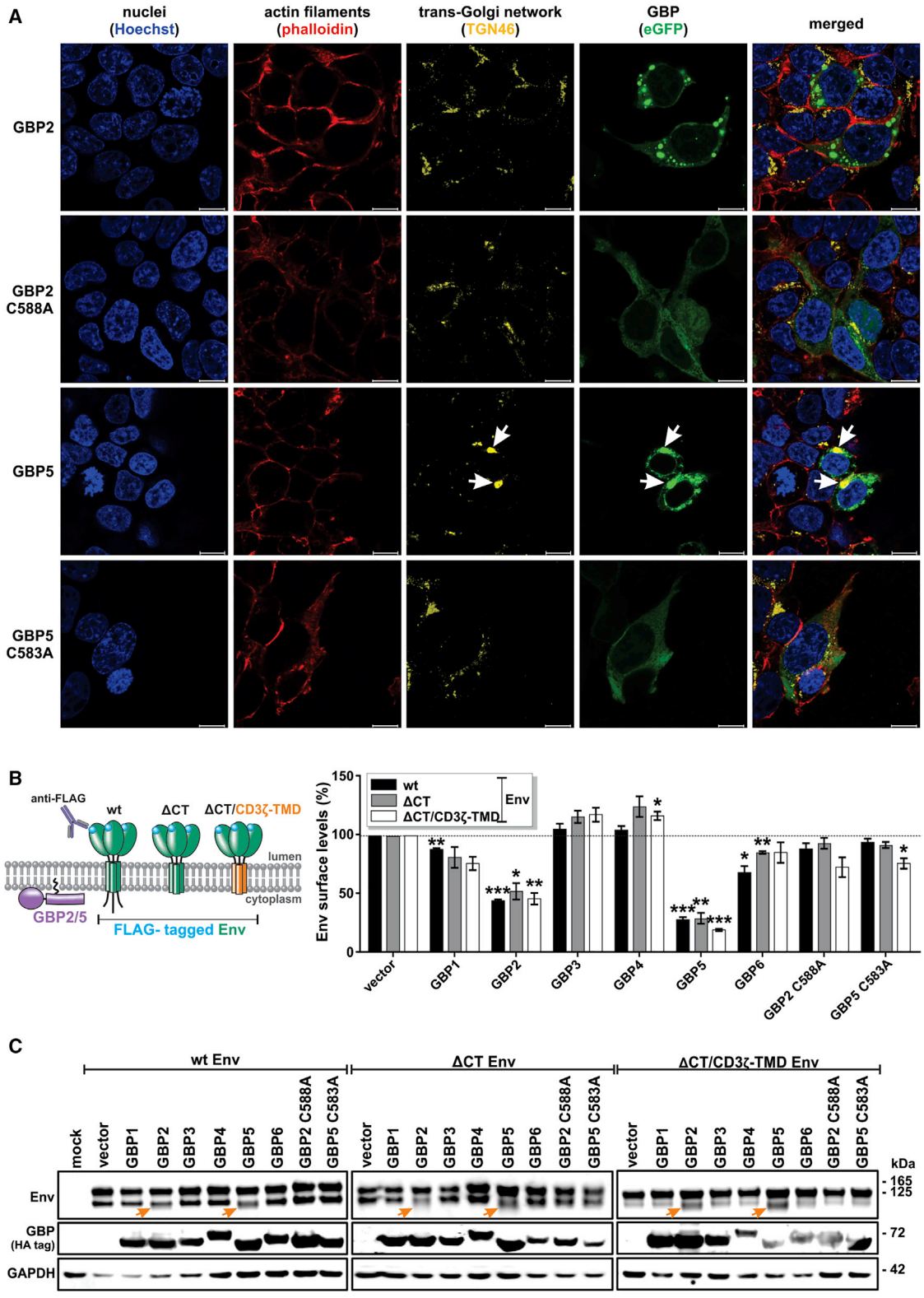

Figure 3. GBP-Mediated Restriction Does Not Involve a Direct Interaction with HIV-1 Env

(A) HEK293T cells were transfected with an expression plasmid for the indicated eGFP-GBP fusion proteins. Two days posttransfection, GBP localization was analyzed by confocal fluorescence microscopy. Nuclei, actin filaments, and the *trans*-Golgi network were stained with Hoechst, phalloidin, and anti-TGN46,

(legend continued on next page)

domain by that of the CD3ζ chain (ΔCT/CD3ζ-TMD) did not abrogate this effect (Figure 3B, right panel). Furthermore, GBP2/5 altered the electrophoretic mobility of both WT and mutant Env proteins (Figure 3C, orange arrows). Thus, GBP2/5 do not directly target Env to suppress its maturation.

GBP2 and GBP5 Reduce the Proteolytic Activity of Furin

Regular processing of the N-glycans in Env and efficient virion incorporation of gp120 depends on furin-mediated cleavage of immature HIV-1 gp160 into mature gp120 and gp41 (Dubay et al., 1995; Moulard and Decroly, 2000). We therefore hypothesized that GBP2/5 might target furin to reduce HIV-1 infectivity. To quantify the catalytically active amount of furin, we took advantage of a reporter substrate (Lamango et al., 1996) harboring the furin target motif Arg-Thr-Lys-Arg (Figure 4A, top) and monitored the release of fluorescent 7-amino-4-methylcoumarin (AMC) over time. Because furin is secreted from the cell (Thimon et al., 2006), we first quantified its activity in the cell culture supernatant, thereby also minimizing a potential bias because of related but non-secreted cytoplasmic proteases (Rousselet et al., 2011; Seidah and Chrétien, 1992). We found that furin activity is significantly reduced in the presence of GBP2/5 (Figures 4A and S4A, left panel). In contrast, the isoprenylation-deficient mutants of GBP2/5 had only marginal effects on furin activity. In cell lysates and in the absence of exogenous furin, the inhibitory effects of GBP2/5 were less pronounced (Figure S4A, right panel), potentially because of the activity of related proteases cleaving the AMC substrate and/or lack of furin inhibition in untransfected bystander cells. Notably, the inhibitory effect of GBP5 decreased with increasing amounts of furin (Figure S4B), suggesting that GBP-mediated restriction may be saturated by high levels of this protease. In agreement with IFNγ-mediated induction of GBP5 (Figure 4B, left panel), IFNγ significantly decreased the catalytically active amount of furin in WT, but not GBP5 knockout THP-1 cells (Figure 4B, right panel). Intriguingly, we also observed a reduced proteolytic processing of furin itself (Figure 4C). Maturation of furin involves a cleavage step, in which the catalytically active domain is separated from the C-terminal transmembrane domain and released into the extracellular space (Figure 4C, middle panel) (Denault et al., 2002; Plaimauer et al., 2001; Thimon et al., 2006). In the presence of GBP2/5, the generation of C-terminal furin fragments (8 and 15 kDa) was significantly reduced (Figures 4C, upper and lower panels). In line with their anti-furin activity, GBP2/5, but not the respective isoprenylation-deficient mutants, reduced processing of gp160 into gp120 in a dose-dependent manner (Figures 4C, upper panel, and 4D). In agreement with a physical association, furin co-immunoprecipitated with GBP2/5 in pull-down assays (Figures 4E and S4C). Notably, GBP2/5 pulled down full-length furin (~90 kDa) and the C-terminal fragments (15 kDa, 8 kDa), but not N-terminal fragments lacking the C terminus. This is in agreement with the hypothesis that GBP2/5 target the cytoplasmic part of furin. Mutation of the C-terminal isoprenylation site abrogated the association of furin with GBP2, but not GBP5. To validate these findings in primary cells, we pulled down endogenous furin from macrophages. The anti-furin antibody co-immunoprecipitated significantly higher quantities of GBP2 and GBP5 than the isotype control (Figure S4D).

Because furin cleaves and activates various cellular factors (Tian et al., 2011), GBP-mediated restriction of HIV-1 may also affect maturation of cellular proteins. Indeed, proteolytic processing of the furin substrates glypican-3 (GPC3) and matrix metalloproteinase-14 (MMP14) (Capurro et al., 2015; Sato et al., 1996) was significantly reduced in the presence of GBP2/5 (Figures 4F and S4E). However, GBPs did not generally interfere with the activity of proteases because HIV-1 Gag was efficiently processed by the viral protease (Figure S4F). In summary, these findings demonstrate that GBP2/5 interfere with HIV-1 infectivity by reducing the maturation and proteolytically active amount of the cellular protease furin.

GBP2 and GBP5 Inhibit Diverse Viral Glycoproteins

Furin is not only a dependency factor for HIV-1, but hijacked by many viral pathogens for the cleavage and maturation of their envelope glycoproteins (Garten et al., 1994; Tian et al., 2011). To determine whether GBP2/5 exert broad antiviral activity, we tested their effect on the infectivity of HIV-1 Δ*env* luciferase reporter viruses pseudotyped with diverse viral glycoproteins. This system allows analysis of the sensitivity of various viral envelope glycoproteins to GBP-mediated restriction in an otherwise identical particle background. Titration experiments revealed that GBP2/5 significantly reduce infectivity of particles carrying glycoproteins of rabies, European bat lyssa, Marburg, highly pathogenic avian influenza A, and murine leukemia viruses in a concentration-dependent manner (Figure 5A). All of these glycoproteins carry cleavage sites that are known or (in case of lyssaviruses) predicted to be processed by furin (Duckert et al., 2004; Sjöberg et al., 2014; Stieneke-Gröber et al., 1992; Volchkov et al., 2000). Interestingly, GBP2/5 also reduced infectivity of viral particles pseudotyped with the glycoprotein of Lassa virus, which is cleaved by PCSK8/SKI (Lenz et al., 2001), a furin-like proprotein convertase that cleaves after non-basic residues. In contrast, viral particles harboring the VSV glycoprotein, which does not require priming by host proteases (Sun et al., 2008; White and Whittaker, 2016), were not affected (Figure 5A). In agreement with an inhibition of furin-mediated glycoprotein

respectively. Scale bar indicates 10 μm. White arrowheads indicate co-localization of GBP5 with TGN46. One representative result of four to six independent experiments is shown.

(B) HEK293T cells were co-transfected with a proviral construct of NL4-3 *env* stop and expression plasmids for the indicated GBPs and FLAG-tagged Env variants. The Env variants lacking the cytoplasmic tail (ΔCT) and/or harboring the transmembrane domain of CD3ζ (ΔCT/CD3ζ-TMD) are schematically depicted on the left. Two days posttransfection, Env levels at the cell surface were determined by flow cytometry using a FLAG-specific antibody. Mean values of three to four independent experiments ± SEM are shown. Asterisks indicate statistically significant differences compared with the vector control.

(C) HEK293T cells were transfected as described in (B). Two days posttransfection, cells were lysed for western blot analysis. Orange arrowheads indicate a reduced apparent molecular weight of cellular gp120 in the presence of GBP2 and GBP5.

See also Figure S3.

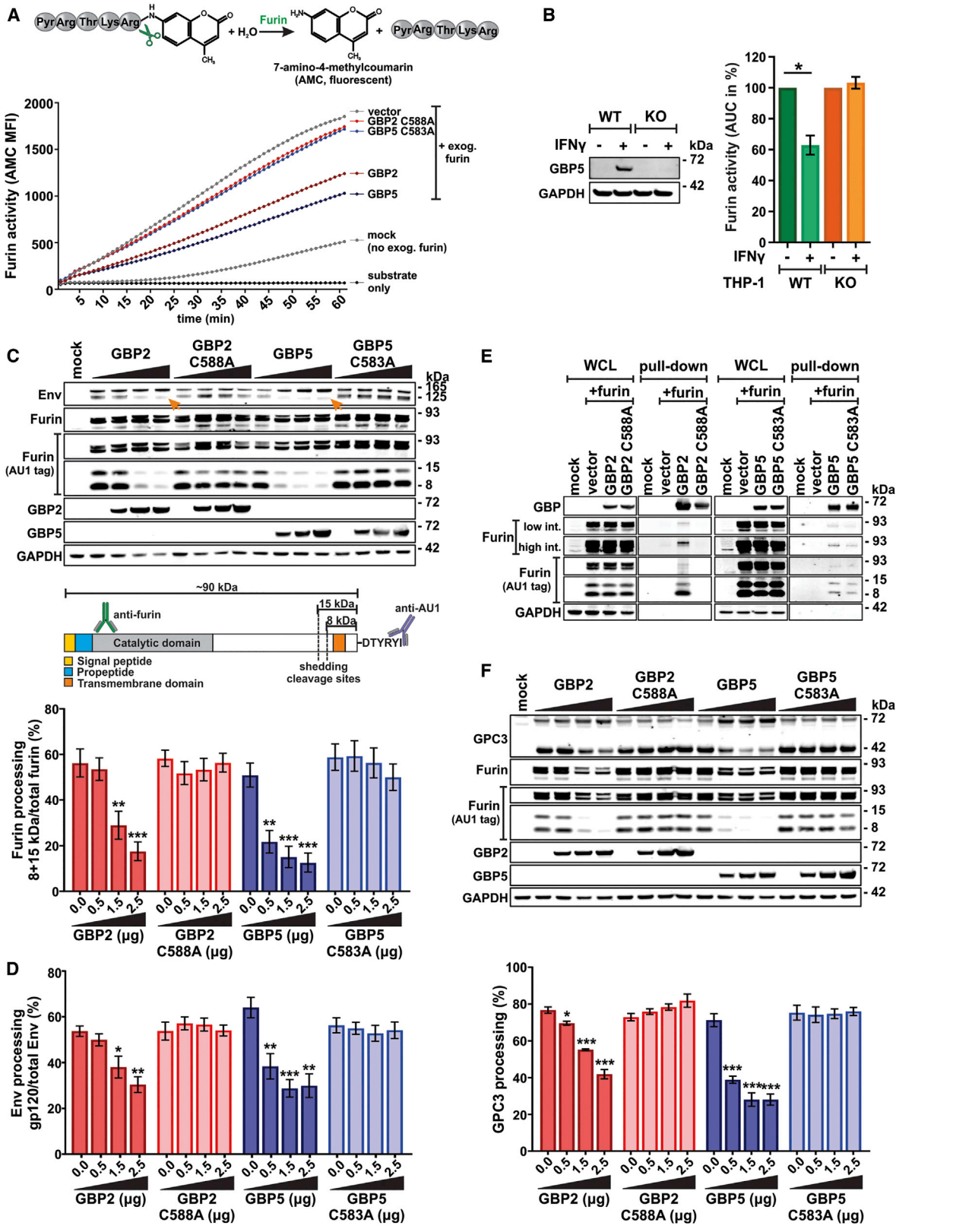

(legend on next page)

processing, GBP5 inhibited the cleavage of MLV gp85 and decreased the incorporation of mature gp70 into viral particles (Figure 5B, left panel). Furthermore, GBP5 suppressed the cleavage of H5N1 influenza A virus HA without affecting viral neuraminidase (NA) levels (Figure 5B, right panel; Figure S5A). Experiments in transfected HEK293T cells and THP-1 knockout cells revealed that GBP2/5 also significantly reduce replication of a Brazilian (Figures 5C and S5B) and an African (Figure 5D) Zika virus strain. Both harbor a furin consensus sequence in their premembrane protein (prM). Similarly, measles and influenza A virus replication were increased upon knockout of GBP5 (Figures 5E and S5C). Thus, GBP2/5 restrict diverse viral pathogens that are dependent on furin-mediated processing of their envelope glycoproteins for full infectivity. Notably, knockout of GBP5 also moderately reduced the inhibitory effect of IFNγ on influenza A virus (Figure 5F), indicating that GBP5 is one of several IFNγ-inducible antiviral factors.

DISCUSSION

GBPs exert a multitude of antiviral, antibacterial, and antiprotozoan activities (Kim et al., 2012; Vestal and Jeyaratnam, 2011). In many cases, however, the underlying inhibitory mechanisms remained unclear. Here, we show that GBP2 and GBP5 target the cellular protease furin, thereby suppressing the maturation and priming of diverse viral glycoproteins, including those of HIV-1, highly pathogenic avian influenza A, murine leukemia, Zika, measles, and Marburg viruses.

Consistent with broad antiviral activity, GBP2 and GBP5 are almost ubiquitously expressed (Uhlén et al., 2015) and may target furin-dependent viral pathogens in a variety of cell types and tissues. Although both GBP2 and GBP5 interfere with viral glycoprotein maturation, they show distinct patterns of subcellular localization. While GBP5 partially co-localizes with the *trans*-Golgi marker TGN46, no such co-localization was observed for GBP2 (Figure 3A). As a result, furin may be targeted at multiple stages of its anterograde transport throughout the cell. GBP2/5 overexpression reduced total furin levels in some experiments (Figure 4F), leaving the possibility that GBP2/5 not only affect furin activity, but also its expression. In agreement with GBP2 and GBP5 complementing each other, the combined knockdown of both proteins in macrophages showed an additive effect on infectious virus production (Figure 2C). Notably, co-expression of several closely related restriction factors with similar inhibitory activities is not uncommon. For example, evolution of SERINC3/5, IFITM1–3, and numerous APOBEC3 proteins may represent a strategy of the host to prevent viral evasion.

Inhibition of furin is a sophisticated strategy to limit viral replication because viruses may not be able to evolve resistance mutations against GBP2/5 because there is no direct interaction of the restriction factor with viral components. Nevertheless, it is tempting to speculate that viruses evolved several mechanisms to overcome GBP-mediated restriction. Dengue virus, for example, does not require complete furin-mediated cleavage of all glycoproteins for efficient infection (Heinz and Stiasny, 2018). Furthermore, some HIV-1 strains acquire mutations in their *vpu* gene that reduce susceptibility to GBP5 by enhancing translation of the viral Env protein (Krapp et al., 2016). Vice versa, certain flaviviruses induce the expression of furin (Presser et al., 2011). Finally, several viruses are able to exploit alternative cellular proteases for maturation of their glycoproteins. For example, some highly pathogenic avian influenza A strains (H5 and H7) contain both a polybasic furin cleavage site and a target sequence for trypsin-like proteases in their HAs (Horimoto et al., 1994; Senne et al., 1996). Notably, the polybasic cleavage site (Arg-X-Arg/Lys-Arg/Lys↓) itself may not only be processed by furin, but also by other members of the proprotein convertase

Figure 4. GBP2 and GBP5 Reduce the Proteolytic Activity of Furin

(A) The conversion of Pyr-Arg-Thr-Lys-Arg-7-amino-4-methylcoumarin (AMC) harboring the furin cleavage site Arg-X-Arg/Lys-Arg/Lys↓ into fluorescent AMC is shown on top. HEK293T cells were co-transfected with an expression plasmid for the indicated GBPs, and an expression plasmid for furin. Two days post-transfection, furin activity in the cell culture supernatants was determined for 60 min after addition of the Pyr-Arg-Thr-Lys-Arg-AMC substrate. Mean values of three independent experiments are shown.

(B) Differentiated THP-1 wild-type (WT) or GBP5 knockout (KO) cells were stimulated with INFγ or left untreated. GBP5 expression was analyzed by western blotting (left panel). Endogenous furin activity in the cell lysates was determined for 30 min after addition of the Pyr-Arg-Thr-Lys-Arg-AMC substrate. The area under the curve (AUC) was calculated and normalized to the unstimulated control (right panel). Mean values of three independent experiments ± SEM are shown. Asterisks indicate significant differences compared with the unstimulated controls (100%).

(C) HEK293T cells were co-transfected with a proviral construct of HIV-1 CH058, increasing amounts of an expression plasmid for the indicated GBPs and an expression plasmid for AU1-tagged furin. Two days posttransfection, cells were lysed for western blot analysis. The upper panel shows one exemplary western blot. Orange arrowheads indicate a reduced apparent molecular weight of cellular gp120. Furin was detected using an antibody directed against the N-terminal catalytic domain (Furin) or an antibody detecting the C-terminal AU1 tag (Furin AU1 tag). In the central panel, a schematic presentation of C-terminally AU1-tagged furin is shown. Binding sites of antibodies used in this study as well as cleavage sites resulting in shedding are indicated. In the lower panel, the ratio of C-terminal furin fragments (8 kDa + 15 kDa) to total furin was calculated. Mean values of seven to nine independent experiments ± SEM are shown.

(D) HEK293T cells were co-transfected and lysed for western blotting as described in (C), and the ratio of gp120 to total Env was calculated. Mean values of four to five independent experiments ± SEM are shown.

(E) HEK293T cells were co-transfected with expression plasmids for AU1-tagged furin and the indicated HA-tagged GBPs. Two days posttransfection, cells were lysed and HA-GBP was immunoprecipitated. The whole-cell lysates (WCLs) and precipitates (pull-down) were analyzed by western blotting. One representative western blot of three to four independent experiments is shown.

(F) HEK293T cells were co-transfected with an expression plasmid for N-terminally HA-tagged glypican-3 (GPC3), increasing amounts of an expression plasmid for the indicated GBPs and an expression plasmid for AU1-tagged furin. Two days posttransfection, cells were lysed for western blot analysis. The upper panel shows one exemplary western blot. In the lower panel, the ratio of cleaved to total GPC3 was calculated. Mean values of three to four independent experiments ± SEM are shown.

In (C), (D), and (F), asterisks indicate statistically significant differences compared with the control without GBP.

See also Figure S4.

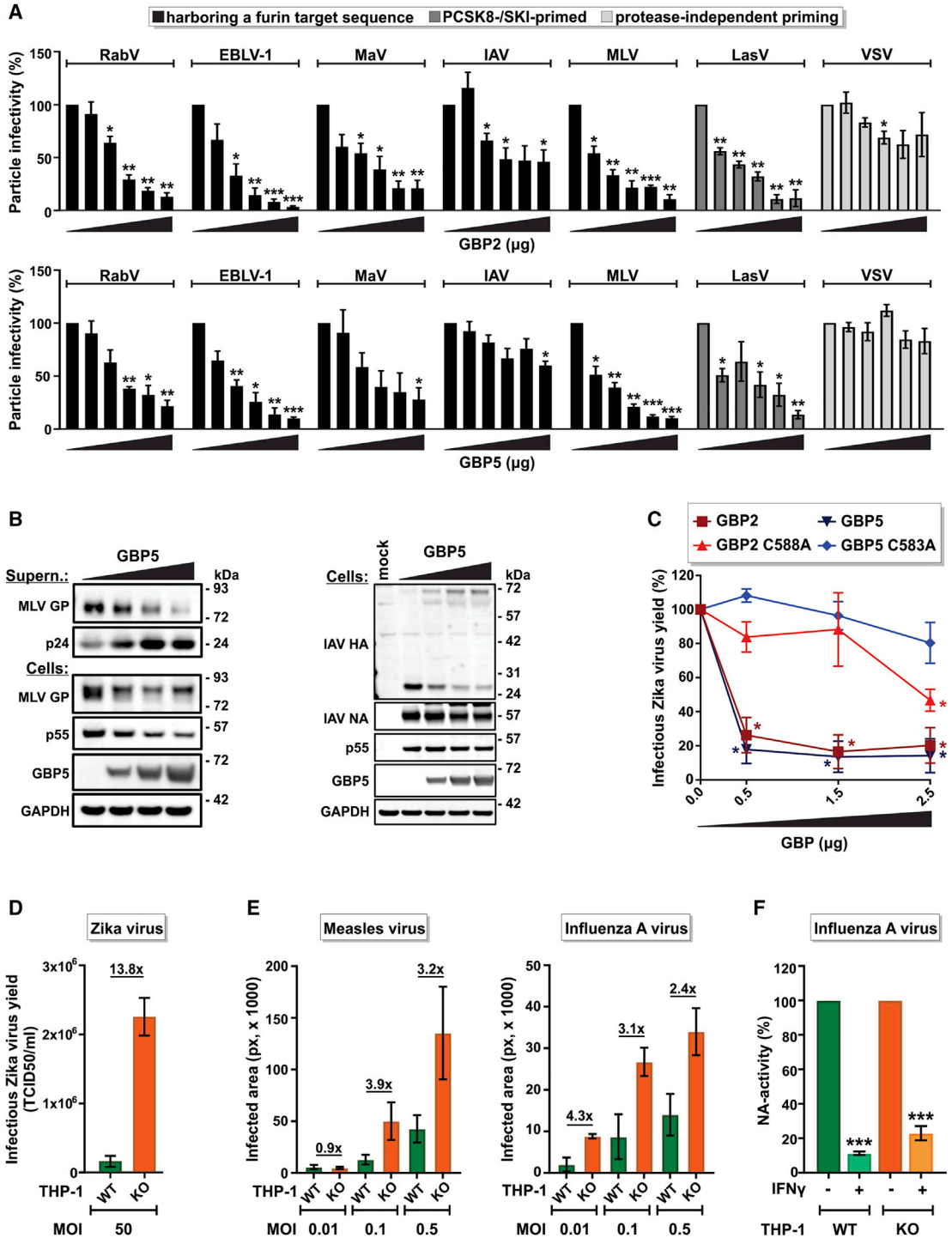

Figure 5. GBP2 and GBP5 Target Diverse Viral Glycoproteins and Inhibit Zika, Measles, and Influenza A Viruses

(A) HEK293T cells were co-transfected with a proviral construct of an HIV-1 NL4-3 *env* stop firefly luciferase reporter virus, increasing amounts (0, 0.25, 0.5, 1.0, 1.5, 2.0 μg) of an expression plasmid for GBP2 (top panel) or GBP5 (bottom panel) and an expression plasmid for the indicated viral glycoproteins: RabV, rabies virus; EBLV-1, European bat lyssavirus 1; MaV, Marburg virus; IAV, influenza A virus; MLV, murine leukemia virus; LasV, Lassa virus; and VSV, vesicular stomatitis virus. Two days posttransfection, supernatants were harvested, and p24 content was determined by ELISA. Furthermore, supernatants were used to infect HEK293T cells. Three days postinfection, a firefly luciferase assay was performed to determine infectious pseudovirus yield. Particle infectivity was determined by normalizing infectious virus yield to the amount of p24. Mean values of three independent experiments ± SEM are shown.

(legend continued on next page)

family (i.e., PCSK1-9) (Duckert et al., 2004). For example, HIV-1 Env can be primed by different proprotein convertases (Decroly et al., 1997; Vollenweider et al., 1996), and it will be interesting to determine whether sequence variations in the cleavage site affect sensitivity of different HIV strains to GBP2/5-mediated restriction. Our finding that GBP2/5 reduce infectivity of viral particles carrying the PCSK8-dependent glycoprotein of Lassa virus (Figure 5A) suggests that the inhibitory effect of GBP2/5 is not limited to furin. Thus, studies on their effect on other proprotein convertases are clearly warranted.

Notably, GBP2/5-mediated inhibition of furin may have relevance beyond viral infections because several bacterial toxins, including anthrax toxin protective antigen and diphtheria toxin, also undergo furin-mediated activation (Gordon et al., 1995). In addition, furin is involved in important cellular processes including the proteolytic activation of cytokines, collagens, hormones, and growth factors (Tian et al., 2011). Indeed, we found that GBP2/5 suppress furin-mediated cleavage of GPC3, a proteoglycan governing cell growth and proliferation (Kandil and Cooper, 2009), and MMP14 (Figures 4F and S4E). Finally, aberrant activation of furin and other proprotein convertases is associated with numerous non-infectious pathological processes including cancer, autoimmune diseases, hypercholesterolemia, dyslexia, and infertility (Seidah and Prat, 2012). These proteases have even been termed "master switches of tumor growth and progression" (Bassi et al., 2005; Seidah and Prat, 2012; Klein-Szanto and Bassi, 2017), and the induction of GBP2/5 by IFNγ may have a protective effect in tumor development and progression. Upon HIV-1 infection, however, GBP protein levels were higher in virally infected cells than in uninfected bystander cells (Figure S2B). Thus, GBP2/5 may primarily interfere with furin-dependent protein maturation in cells that are lost to viral infection anyway. In contrast, uninfected bystander cells may exhibit normal furin activity and are protected by the reduced infectivity of newly formed virions.

In summary, we identified a broadly effective antiviral mechanism involving the inhibition of a cellular dependency factor that is hijacked by many viral pathogens. Our finding that GBP2/5 display broad antiviral activity by targeting the cellular protease furin also helps to explain previously reported effects of GBPs on viral replication. Future experiments will reveal whether GBP2/5 inhibit the activity of additional proteases, and it will be of interest to further determine the relevance of GBP2/5 in regulating the processing of cellular proteins in health and disease.

STAR★METHODS

Detailed methods are provided in the online version of this paper and include the following:

- KEY RESOURCES TABLE
- CONTACT FOR REAGENT AND RESOURCE SHARING
- EXPERIMENTAL MODEL AND SUBJECT DETAILS
  - Cell lines
  - Primary cell cultures
- METHOD DETAILS
  - Generation of GBP/furin expression plasmids
  - Generation of Env expression plasmids
  - Generation of HIV-1 chimeras expressing GBP2/5
  - Transfections and generation of virus stocks
  - Generation of a measles virus GFP reporter virus
  - Generation of measles and influenza virus stocks
  - Titer determination of measles and influenza virus stocks
  - Infection of TZM-bl reporter cells
  - Stimulation of primary cells
  - Infection of primary cells
  - siRNA transfection and infection of macrophages
  - Infection of THP-1 cells with measles, influenza A and Zika viruses
  - ELISA
  - Flow cytometry
  - MUNANA assay
  - Cell viability assay
  - Western blotting
  - Co-immunoprecipitation
  - Microscopy
  - 4G2 immunostaining
  - Furin activity assay
  - Proteolytic processing of GPC3 and MMP14
  - Firefly luciferase assay

(B) HEK293T cells were co-transfected with a proviral construct of HIV-1 NL4-3 *env* stop, increasing amounts (0, 0.5, 1.5, 2.5 μg) of an expression plasmid for GBP5 and an expression plasmid for the indicated viral glycoproteins. Two days posttransfection, cells and supernatants were lysed for western blot analysis. One representative western blot of three independent experiments is shown.
(C) HEK293T cells were co-transfected with a BAC clone of the Brazilian Zika virus isolate SPH2015 and increasing amounts of an expression plasmid for the indicated GBPs. Two days posttransfection, supernatants were harvested and infectious virus yield was determined by infection of Vero E6 cells and subsequent staining of ZIKV-E. Mean values of three independent experiments ± SEM are shown.
(D) Differentiated THP-1 WT or GBP5 KO cells were infected with the African Zika virus isolate MR766. Four days post infection, supernatants were harvested and infectious virus yield was determined by serial dilution infection of Vero E6 cells and subsequent median tissue culture infectious dose ($TCID_{50}$) determination. Mean values of three independent experiments ± SEM are shown. Number indicates n-fold increase.
(E) Differentiated and IFNγ-stimulated THP-1 WT or GBP5 KO cells were infected with GFP-expressing measles virus (strain Schwarz) (left panel) or influenza A virus (strain SC35M) (right panel). 48 h (measles virus) or 24 h (influenza A virus) post infection, viral gene expression was analyzed by determining GFP expression with a Cytation3 imaging reader. Mean values of three independent experiments ± SEM are shown. Numbers indicate n-fold increase.
(F) Differentiated THP-1 WT or GBP5 KO cells were stimulated with INFγ or left untreated and infected (MOI of 0.01) with influenza A virus (strain SC35M). 24 h post infection, neuraminidase activity was determined by a MUNANA assay. Mean values of four independent experiments ± SEM are shown. Asterisks indicate significant differences compared with the unstimulated control, which was set to 100%.
In (A) and (C), asterisks indicate statistically significant differences compared with the control without GBP.
See also Figure S5.

- QUANTIFICATION AND STATISTICAL ANALYSIS
- ADDITIONAL RESOURCES

SUPPLEMENTAL INFORMATION

Supplemental Information can be found online at https://doi.org/10.1016/j.celrep.2019.04.063.

ACKNOWLEDGMENTS

We thank Martha Mayer, Regina Linsenmeyer, Kerstin Regensburger, Susanne Engelhart, and Daniela Krnavek for excellent technical assistance, as well as Franziska Krüger and Dorota Kmiec for support with microscopic analyses and protein-protein interaction assays, respectively. We also thank Beatrice H. Hahn and Vicente Planelles for providing proviral HIV-1 clones, Stephan Becker and Christine Goffinet for expression plasmids, and Thomas Hoffmann and Johannes Döscher as well as the Bundeswehr Hospital Ulm for providing tonsils. Furthermore, we thank Martin Schwemmle for providing influenza A virus stocks and Christian Buchholz for providing MLV gp70 antiserum. Finally, we thank James B. Munro for advice regarding the insertion of a FLAG-tag in Env. This work was funded by Ulm University starting grants "Baustein 3.2" to D.H. and J.A.M.; the DFG priority program "Innate Sensing and Restriction of Retroviruses" (SPP 1923) to K.S., U.D., O.T.F., F.K., and D.S.; the DFG TRR83 (project 15) to O.T.F.; and DFG Ki548/16 to F.K. F.Z. and F.K. are supported by the Collaborative Research Centre CRC1279 of the DFG. J.A.M. is indebted to the Baden-Württemberg Stiftung for financial support of this research project by the Elite programme for postdoctoral researchers. K.M.J.S. was supported by a Marie Skłodowska-Curie Individual Fellowship from the European Union's Framework Program for Research and Innovation Horizon 2020 (2014-2020) under the Grant Agreement No. 794803 ("VIAR"), and K.-K.C. by the DFG TRR 237. E.B., L.K., F.Z., R.G., and E.H. were supported by the International Graduate School in Molecular Medicine Ulm (IGradU).

AUTHOR CONTRIBUTIONS

D.S., E.B., D.H., and F.K. conceptualized the study and designed the experiments. E.B. and D.H. performed most of the experiments. L.K. analyzed the inducibility of GBPs in $CD4^+$ T cells. F.Z. tested the effect of GBPs on infectivity of lentiviral pseudoparticles. R.G. tested the effect of GBPs on Zika virus replication. K.M.J.S. generated measles and influenza virus stocks. C.K.P. and K.-K.C. generated and characterized the GFP-expressing measles virus clone. E.H. established the 4-(methylumbelliferyl)-N-acetylneuraminic acid (MUNANA) assay. M.W., S.P., and G.S. generated and characterized the Zika virus clone SPH2015. R.G., J.A.M., and J.M. established assays to quantify infectious Zika virus production. E.B. and R.W. performed microscopic analyses. K.S. and U.D. generated and provided different IFNα subtypes. M.R.J. generated and provided THP-1 knockout cells. E.B., D.H., and D.S. prepared the figures, and D.S. wrote the initial draft of the manuscript. All authors reviewed and edited the manuscript. D.H., U.D., O.T.F., F.K., and D.S. provided resources and acquired funding.

DECLARATION OF INTERESTS

The authors declare no competing interests.

Received: October 19, 2018
Revised: March 11, 2019
Accepted: April 12, 2019
Published: May 14, 2019

REFERENCES

Abraham, S., Choi, J.-G., Ortega, N.M., Zhang, J., Shankar, P., and Swamy, N.M. (2016). Gene therapy with plasmids encoding IFN-β or IFN-α14 confers long-term resistance to HIV-1 in humanized mice. Oncotarget *7*, 78412–78420.

Anderson, S.L., Carton, J.M., Lou, J., Xing, L., and Rubin, B.Y. (1999). Interferon-induced guanylate binding protein-1 (GBP-1) mediates an antiviral effect against vesicular stomatitis virus and encephalomyocarditis virus. Virology *256*, 8–14.

Bassi, D.E., Fu, J., Lopez de Cicco, R., and Klein-Szanto, A.J.P. (2005). Proprotein convertases: "master switches" in the regulation of tumor growth and progression. Mol. Carcinog. *44*, 151–161.

Britzen-Laurent, N., Bauer, M., Berton, V., Fischer, N., Syguda, A., Reipschläger, S., Naschberger, E., Herrmann, C., and Stürzl, M. (2010). Intracellular trafficking of guanylate-binding proteins is regulated by heterodimerization in a hierarchical manner. PLoS ONE *5*, e14246.

Capurro, M., Shi, W., Izumikawa, T., Kitagawa, H., and Filmus, J. (2015). Processing by convertases is required for glypican-3-induced inhibition of Hedgehog signaling. J. Biol. Chem. *290*, 7576–7585.

Cheng, Y.S., Colonno, R.J., and Yin, F.H. (1983). Interferon induction of fibroblast proteins with guanylate binding activity. J. Biol. Chem. *258*, 7746–7750.

Chowers, M.Y., Spina, C.A., Kwoh, T.J., Fitch, N.J., Richman, D.D., and Guatelli, J.C. (1994). Optimal infectivity in vitro of human immunodeficiency virus type 1 requires an intact nef gene. J. Virol. *68*, 2906–2914.

Coffey, L.L., Pesavento, P.A., Keesler, R.I., Singapuri, A., Watanabe, J., Watanabe, R., Yee, J., Bliss-Moreau, E., Cruzen, C., Christe, K.L., et al. (2017). Zika Virus Tissue and Blood Compartmentalization in Acute Infection of Rhesus Macaques. PLoS ONE *12*, e0171148.

Connor, R.I., Chen, B.K., Choe, S., and Landau, N.R. (1995). Vpr is required for efficient replication of human immunodeficiency virus type-1 in mononuclear phagocytes. Virology *206*, 935–944.

Coppola, J.M., Bhojani, M.S., Ross, B.D., and Rehemtulla, A. (2008). A small-molecule furin inhibitor inhibits cancer cell motility and invasiveness. Neoplasia *10*, 363–370.

Corpet, F., Gouzy, J., and Kahn, D. (1999). Browsing protein families via the "Rich Family Description" format. Bioinforma. Oxf. Engl. *15*, 1020–1027.

Cunha, M.S., Esposito, D.L.A., Rocco, I.M., Maeda, A.Y., Vasami, F.G.S., Nogueira, J.S., de Souza, R.P., Suzuki, A., Addas-Carvalho, M., Barjas-Castro, M. de L., et al. (2016). First Complete Genome Sequence of Zika Virus (Flaviviridae, Flavivirus) from an Autochthonous Transmission in Brazil. Genome Announc. *4*, e00032-e16.

Decker, T., Lew, D.J., Cheng, Y.S., Levy, D.E., and Darnell, J.E., Jr. (1989). Interactions of alpha- and gamma-interferon in the transcriptional regulation of the gene encoding a guanylate-binding protein. EMBO J. *8*, 2009–2014.

Decroly, E., Benjannet, S., Savaria, D., and Seidah, N.G. (1997). Comparative functional role of PC7 and furin in the processing of the HIV envelope glycoprotein gp160. FEBS Lett. *405*, 68–72.

del Valle, J.R., Devaux, P., Hodge, G., Wegner, N.J., McChesney, M.B., and Cattaneo, R. (2007). A vectored measles virus induces hepatitis B surface antigen antibodies while protecting macaques against measles virus challenge. J. Virol. *81*, 10597–10605.

Denault, J., Bissonnette, L., Longpré, J., Charest, G., Lavigne, P., and Leduc, R. (2002). Ectodomain shedding of furin: kinetics and role of the cysteine-rich region. FEBS Lett. *527*, 309–314.

Dubay, J.W., Dubay, S.R., Shin, H.J., and Hunter, E. (1995). Analysis of the cleavage site of the human immunodeficiency virus type 1 glycoprotein: requirement of precursor cleavage for glycoprotein incorporation. J. Virol. *69*, 4675–4682.

DuBridge, R.B., Tang, P., Hsia, H.C., Leong, P.M., Miller, J.H., and Calos, M.P. (1987). Analysis of mutation in human cells by using an Epstein-Barr virus shuttle system. Mol. Cell. Biol. *7*, 379–387.

Duckert, P., Brunak, S., and Blom, N. (2004). Prediction of proprotein convertase cleavage sites. Protein Eng. Des. Sel. *17*, 107–112.

Federici, T., Kutner, R., Zhang, X.-Y., Kuroda, H., Tordo, N., Boulis, N.M., and Reiser, J. (2009). Comparative analysis of HIV-1-based lentiviral vectors bearing lyssavirus glycoproteins for neuronal gene transfer. Genet. Vaccines Ther. *7*, 1.

Fenton-May, A.E., Dibben, O., Emmerich, T., Ding, H., Pfafferott, K., Aasa-Chapman, M.M., Pellegrino, P., Williams, I., Cohen, M.S., Gao, F., et al. (2013). Relative resistance of HIV-1 founder viruses to control by interferon-alpha. Retrovirology *10*, 146.

Fouchier, R.A., Meyer, B.E., Simon, J.H., Fischer, U., and Malim, M.H. (1997). HIV-1 infection of non-dividing cells: evidence that the amino-terminal basic region of the viral matrix protein is important for Gag processing but not for post-entry nuclear import. EMBO J. *16*, 4531–4539.

Freel, S.A., Picking, R.A., Ferrari, G., Ding, H., Ochsenbauer, C., Kappes, J.C., Kirchherr, J.L., Soderberg, K.A., Weinhold, K.J., Cunningham, C.K., et al. (2012). Initial HIV-1 antigen-specific CD8+ T cells in acute HIV-1 infection inhibit transmitted/founder virus replication. J. Virol. *86*, 6835–6846.

Gao, F., Scearce, R.M., Alam, S.M., Hora, B., Xia, S., Hohm, J.E., Parks, R.J., Ogburn, D.F., Tomaras, G.D., Park, E., et al. (2009). Cross-reactive monoclonal antibodies to multiple HIV-1 subtype and SIVcpz envelope glycoproteins. Virology *394*, 91–98.

Garten, W., Hallenberger, S., Ortmann, D., Schäfer, W., Vey, M., Angliker, H., Shaw, E., and Klenk, H.D. (1994). Processing of viral glycoproteins by the subtilisin-like endoprotease furin and its inhibition by specific peptidylchloroalkylketones. Biochimie *76*, 217–225.

Ghanem, A., Kern, A., and Conzelmann, K.-K. (2012). Significantly improved rescue of rabies virus from cDNA plasmids. Eur. J. Cell Biol. *91*, 10–16.

Girdlestone, J., and Wing, M. (1996). Autocrine activation by interferon-gamma of STAT factors following T cell activation. Eur. J. Immunol. *26*, 704–709.

Gordon, V.M., Klimpel, K.R., Arora, N., Henderson, M.A., and Leppla, S.H. (1995). Proteolytic activation of bacterial toxins by eukaryotic cells is performed by furin and by additional cellular proteases. Infect. Immun. *63*, 82–87.

Haller, O., Staeheli, P., Schwemmle, M., and Kochs, G. (2015). Mx GTPases: dynamin-like antiviral machines of innate immunity. Trends Microbiol. *23*, 154–163.

Harper, M.S., Guo, K., Gibbert, K., Lee, E.J., Dillon, S.M., Barrett, B.S., McCarter, M.D., Hasenkrug, K.J., Dittmer, U., Wilson, C.C., and Santiago, M.L. (2015). Interferon-α Subtypes in an Ex Vivo Model of Acute HIV-1 Infection: Expression, Potency and Effector Mechanisms. PLoS Pathog. *11*, e1005254.

Heinz, F.X., and Stiasny, K. (2018). Proteolytic activation of flavivirus envelope proteins. In Activation of Viruses by Host Proteases, E. Böttcher-Friebertshäuser, W. Garten, and H.D. Klenk, eds. (Springer), pp. 109–132.

Horimoto, T., Nakayama, K., Smeekens, S.P., and Kawaoka, Y. (1994). Proprotein-processing endoproteases PC6 and furin both activate hemagglutinin of virulent avian influenza viruses. J. Virol. *68*, 6074–6078.

Hotter, D., Sauter, D., and Kirchhoff, F. (2017). Guanylate binding protein 5: Impairing virion infectivity by targeting retroviral envelope glycoproteins. Small GTPases *8*, 31–37.

Itsui, Y., Sakamoto, N., Kurosaki, M., Kanazawa, N., Tanabe, Y., Koyama, T., Takeda, Y., Nakagawa, M., Kakinuma, S., Sekine, Y., et al. (2006). Expressional screening of interferon-stimulated genes for antiviral activity against hepatitis C virus replication. J. Viral Hepat. *13*, 690–700.

Itsui, Y., Sakamoto, N., Kakinuma, S., Nakagawa, M., Sekine-Osajima, Y., Tasaka-Fujita, M., Nishimura-Sakurai, Y., Suda, G., Karakama, Y., Mishima, K., et al. (2009). Antiviral effects of the interferon-induced protein guanylate binding protein 1 and its interaction with the hepatitis C virus NS5B protein. Hepatology *50*, 1727–1737.

Kandil, D.H., and Cooper, K. (2009). Glypican-3: a novel diagnostic marker for hepatocellular carcinoma and more. Adv. Anat. Pathol. *16*, 125–129.

Kim, B.-H., Shenoy, A.R., Kumar, P., Bradfield, C.J., and MacMicking, J.D. (2012). IFN-inducible GTPases in host cell defense. Cell Host Microbe *12*, 432–444.

Klein-Szanto, A.J., and Bassi, D.E. (2017). Proprotein convertase inhibition: Paralyzing the cell's master switches. Biochem. Pharmacol. *140*, 8–15.

Krapp, C., Hotter, D., Gawanbacht, A., McLaren, P.J., Kluge, S.F., Stürzel, C.M., Mack, K., Reith, E., Engelhart, S., Ciuffi, A., et al. (2016). Guanylate Binding Protein (GBP) 5 Is an Interferon-Inducible Inhibitor of HIV-1 Infectivity. Cell Host Microbe *19*, 504–514.

Lamango, N.S., Zhu, X., and Lindberg, I. (1996). Purification and enzymatic characterization of recombinant prohormone convertase 2: stabilization of activity by 21 kDa 7B2. Arch. Biochem. Biophys. *330*, 238–250.

Lavender, K.J., Gibbert, K., Peterson, K.E., Van Dis, E., Francois, S., Woods, T., Messer, R.J., Gawanbacht, A., Müller, J.A., Münch, J., et al. (2016). Interferon Alpha Subtype-Specific Suppression of HIV-1 Infection In Vivo. J. Virol. *90*, 6001–6013.

Lenz, O., ter Meulen, J., Klenk, H.D., Seidah, N.G., and Garten, W. (2001). The Lassa virus glycoprotein precursor GP-C is proteolytically processed by subtilase SKI-1/S1P. Proc. Natl. Acad. Sci. USA *98*, 12701–12705.

Lew, D.J., Decker, T., Strehlow, I., and Darnell, J.E. (1991). Overlapping elements in the guanylate-binding protein gene promoter mediate transcriptional induction by alpha and gamma interferons. Mol. Cell. Biol. *11*, 182–191.

Moulard, M., and Decroly, E. (2000). Maturation of HIV envelope glycoprotein precursors by cellular endoproteases. Biochim. Biophys. Acta *1469*, 121–132.

Münch, J., Rajan, D., Rücker, E., Wildum, S., Adam, N., and Kirchhoff, F. (2005). The role of upstream U3 sequences in HIV-1 replication and CD4+ T cell depletion in human lymphoid tissue ex vivo. Virology *341*, 313–320.

Munro, J.B., Gorman, J., Ma, X., Zhou, Z., Arthos, J., Burton, D.R., Koff, W.C., Courter, J.R., Smith, A.B., 3rd, Kwong, P.D., et al. (2014). Conformational dynamics of single HIV-1 envelope trimers on the surface of native virions. Science *346*, 759–763.

Nordmann, A., Wixler, L., Boergeling, Y., Wixler, V., and Ludwig, S. (2012). A new splice variant of the human guanylate-binding protein 3 mediates anti-influenza activity through inhibition of viral transcription and replication. FASEB J. *26*, 1290–1300.

Ochsenbauer, C., Edmonds, T.G., Ding, H., Keele, B.F., Decker, J., Salazar, M.G., Salazar-Gonzalez, J.F., Shattock, R., Haynes, B.F., Shaw, G.M., et al. (2012). Generation of transmitted/founder HIV-1 infectious molecular clones and characterization of their replication capacity in CD4 T lymphocytes and monocyte-derived macrophages. J. Virol. *86*, 2715–2728.

Olszewski, M.A., Gray, J., and Vestal, D.J. (2006). In silico genomic analysis of the human and murine guanylate-binding protein (GBP) gene clusters. J. Interferon Cytokine Res. *26*, 328–352.

Parrish, N.F., Gao, F., Li, H., Giorgi, E.E., Barbian, H.J., Parrish, E.H., Zajic, L., Iyer, S.S., Decker, J.M., Kumar, A., et al. (2013). Phenotypic properties of transmitted founder HIV-1. Proc. Natl. Acad. Sci. USA *110*, 6626–6633.

Plaimauer, B., Mohr, G., Wernhart, W., Himmelspach, M., Dorner, F., and Schlokat, U. (2001). 'Shed' furin: mapping of the cleavage determinants and identification of its C-terminus. Biochem. J. *354*, 689–695.

Platt, E.J., Wehrly, K., Kuhmann, S.E., Chesebro, B., and Kabat, D. (1998). Effects of CCR5 and CD4 cell surface concentrations on infections by macrophagetropic isolates of human immunodeficiency virus type 1. J. Virol. *72*, 2855–2864.

Presser, L.D., Haskett, A., and Waris, G. (2011). Hepatitis C virus-induced furin and thrombospondin-1 activate TGF-β1: role of TGF-β1 in HCV replication. Virology *412*, 284–296.

Radecke, F., Spielhofer, P., Schneider, H., Kaelin, K., Huber, M., Dötsch, C., Christiansen, G., and Billeter, M.A. (1995). Rescue of measles viruses from cloned DNA. EMBO J. *14*, 5773–5784.

Reuther, P., Göpfert, K., Dudek, A.H., Heiner, M., Herold, S., and Schwemmle, M. (2015). Generation of a variety of stable Influenza A reporter viruses by genetic engineering of the NS gene segment. Sci. Rep. *5*, 11346.

Rousselet, E., Benjannet, S., Hamelin, J., Canuel, M., and Seidah, N.G. (2011). The proprotein convertase PC7: unique zymogen activation and trafficking pathways. J. Biol. Chem. *286*, 2728–2738.

Rowland, R.R.R., Lunney, J., and Dekkers, J. (2012). Control of porcine reproductive and respiratory syndrome (PRRS) through genetic improvements in disease resistance and tolerance. Front. Genet. *3*, 260.

Runge, S., Sparrer, K.M.J., Lässig, C., Hembach, K., Baum, A., García-Sastre, A., Söding, J., Conzelmann, K.-K., and Hopfner, K.-P. (2014). In vivo ligands of MDA5 and RIG-I in measles virus-infected cells. PLoS Pathog. *10*, e1004081.

Salazar-Gonzalez, J.F., Salazar, M.G., Keele, B.F., Learn, G.H., Giorgi, E.E., Li, H., Decker, J.M., Wang, S., Baalwa, J., Kraus, M.H., et al. (2009). Genetic identity, biological phenotype, and evolutionary pathways of transmitted/founder viruses in acute and early HIV-1 infection. J. Exp. Med. *206*, 1273–1289.

Sato, H., Kinoshita, T., Takino, T., Nakayama, K., and Seiki, M. (1996). Activation of a recombinant membrane type 1-matrix metalloproteinase (MT1-MMP) by furin and its interaction with tissue inhibitor of metalloproteinases (TIMP)-2. FEBS Lett. *393*, 101–104.

Schmier, S., Mostafa, A., Haarmann, T., Bannert, N., Ziebuhr, J., Veljkovic, V., Dietrich, U., and Pleschka, S. (2015). In Silico Prediction and Experimental Confirmation of HA Residues Conferring Enhanced Human Receptor Specificity of H5N1 Influenza A Viruses. Sci. Rep. *5*, 11434.

Seidah, N.G., and Chrétien, M. (1992). Proprotein and prohormone convertases of the subtilisin family Recent developments and future perspectives. Trends Endocrinol. Metab. *3*, 133–140.

Seidah, N.G., and Prat, A. (2012). The biology and therapeutic targeting of the proprotein convertases. Nat. Rev. Drug Discov. *11*, 367–383.

Senne, D.A., Panigrahy, B., Kawaoka, Y., Pearson, J.E., Süss, J., Lipkind, M., Kida, H., and Webster, R.G. (1996). Survey of the hemagglutinin (HA) cleavage site sequence of H5 and H7 avian influenza viruses: amino acid sequence at the HA cleavage site as a marker of pathogenicity potential. Avian Dis. *40*, 425–437.

Simmons, G., Reeves, J.D., Grogan, C.C., Vandenberghe, L.H., Baribaud, F., Whitbeck, J.C., Burke, E., Buchmeier, M.J., Soilleux, E.J., Riley, J.L., et al. (2003). DC-SIGN and DC-SIGNR bind ebola glycoproteins and enhance infection of macrophages and endothelial cells. Virology *305*, 115–123.

Sjöberg, M., Wu, S.-R., Löving, R., Rantalainen, K., Lindqvist, B., and Garoff, H. (2014). Furin cleavage of the Moloney murine leukemia virus Env precursor reorganizes the spike structure. Proc. Natl. Acad. Sci. USA *111*, 6034–6039.

Staeheli, P., Prochazka, M., Steigmeier, P.A., and Haller, O. (1984). Genetic control of interferon action: mouse strain distribution and inheritance of an induced protein with guanylate-binding property. Virology *137*, 135–142.

Stieneke-Gröber, A., Vey, M., Angliker, H., Shaw, E., Thomas, G., Roberts, C., Klenk, H.D., and Garten, W. (1992). Influenza virus hemagglutinin with multibasic cleavage site is activated by furin, a subtilisin-like endoprotease. EMBO J. *11*, 2407–2414.

Sun, X., Belouzard, S., and Whittaker, G.R. (2008). Molecular architecture of the bipartite fusion loops of vesicular stomatitis virus glycoprotein G, a class III viral fusion protein. J. Biol. Chem. *283*, 6418–6427.

Thimon, V., Belghazi, M., Dacheux, J.-L., and Gatti, J.-L. (2006). Analysis of furin ectodomain shedding in epididymal fluid of mammals: demonstration that shedding of furin occurs in vivo. Reproduction *132*, 899–908.

Tian, S., Huang, Q., Fang, Y., and Wu, J. (2011). FurinDB: A database of 20-residue furin cleavage site motifs, substrates and their associated drugs. Int. J. Mol. Sci. *12*, 1060–1065.

Uhlén, M., Fagerberg, L., Hallström, B.M., Lindskog, C., Oksvold, P., Mardinoglu, A., Sivertsson, Å., Kampf, C., Sjöstedt, E., Asplund, A., et al. (2015). Proteomics. Tissue-based map of the human proteome. Science *347*, 1260419.

Vestal, D.J., and Jeyaratnam, J.A. (2011). The guanylate-binding proteins: emerging insights into the biochemical properties and functions of this family of large interferon-induced guanosine triphosphatase. J. Interferon Cytokine Res. *31*, 89–97.

Veugelers, M., Cat, B.D., Muyldermans, S.Y., Reekmans, G., Delande, N., Frints, S., Legius, E., Fryns, J.P., Schrander-Stumpel, C., Weidle, B., et al. (2000). Mutational analysis of the GPC3/GPC4 glypican gene cluster on Xq26 in patients with Simpson-Golabi-Behmel syndrome: identification of loss-of-function mutations in the GPC3 gene. Hum. Mol. Genet. *9*, 1321–1328.

Volchkov, V.E., Volchkova, V.A., Stroher, U., Becker, S., Dolnik, O., Cieplik, M., Garten, W., Klenk, H.D., and Feldmann, H. (2000). Proteolytic processing of Marburg virus glycoprotein. Virology *268*, 1–6.

Vollenweider, F., Benjannet, S., Decroly, E., Savaria, D., Lazure, C., Thomas, G., Chrétien, M., and Seidah, N.G. (1996). Comparative cellular processing of the human immunodeficiency virus (HIV-1) envelope glycoprotein gp160 by the mammalian subtilisin/kexin-like convertases. Biochem. J. *314*, 521–532.

Wenigenrath, J., Kolesnikova, L., Hoenen, T., Mittler, E., and Becker, S. (2010). Establishment and application of an infectious virus-like particle system for Marburg virus. J. Gen. Virol. *91*, 1325–1334.

White, J.M., and Whittaker, G.R. (2016). Fusion of Enveloped Viruses in Endosomes. Traffic *17*, 593–614.

Wildum, S., Schindler, M., Münch, J., and Kirchhoff, F. (2006). Contribution of Vpu, Env, and Nef to CD4 down-modulation and resistance of human immunodeficiency virus type 1-infected T cells to superinfection. J. Virol. *80*, 8047–8059.

Zimmerman, E.S., Sherman, M.P., Blackett, J.L., Neidleman, J.A., Kreis, C., Mundt, P., Williams, S.A., Warmerdam, M., Kahn, J., Hecht, F.M., et al. (2006). Human immunodeficiency virus type 1 Vpr induces DNA replication stress in vitro and in vivo. J. Virol. *80*, 10407–10418.

STAR★METHODS

KEY RESOURCES TABLE

REAGENT or RESOURCE	SOURCE	IDENTIFIER
Antibodies		
Mouse monoclonal anti-GBP2	Santa Cruz	Cat# sc-271568; RRID:AB_10655677
Goat monoclonal anti-GBP5	Santa Cruz	Cat# sc-160353; RRID:AB_2247449
Rabbit polyclonal anti-Furin	Abcam	Cat# ab28547; RRID:AB_732450
Mouse monoclonal anti-HA tag	Abcam	Cat# ab18181; RRID:AB_444303
Rabbit polyclonal anti-AU1 tag	Novus Biologicals	Cat# NB600-453; RRID:AB_10003439
Rabbit monoclonal anti-V5 tag	Cell Signaling	Cat# 13202; RRID:AB_2687461
Sheep polyclonal anti-TGN46	Bio-Rad	Cat# AHP500G; RRID:AB_323104
Rabbit polyclonal anti-GFP	Abcam	Cat# ab290; RRID:AB_303395
Rabbit polyclonal anti-GAPDH	BioLegend	Cat# 631401; RRID: AB_2247301
Mouse monoclonal anti-β-actin	Abcam	Cat# ab8226; RRID:AB_306371
Mouse monoclonal anti-CD4 Per-CP	Beckman Coulter	Cat# 550631; RRID:AB_393791
Mouse monoclonal anti-CD11 FITC	Abcam	Cat# ab22540
Mouse monoclonal anti-Env	NIH, Gao et al., 2009	Cat# 12559
Goat anti-Rauscher MLV gp70 antiserum	Christian Buchholz	N/A
Mouse monoclonal anti-p24	Abcam	Cat# ab9071; RRID: AB_306981
Rabbit polyclonal isotype control	Abcam	Cat# ab37415; RRID: AB_2631996
Mouse anti-HIV-1 core antigen FITC (clone KC57)	Beckman Coulter	Cat# 6604665; RRID:AB_1575987
Rat monoclonal anti-FLAG APC	BioLegend	Cat# 637307; RRID:AB_2561496
Mouse monoclonal anti-flavivirus group antigen 4G2	Absolute Antibody	Cat# Ab00230-2.0; RRID: AB_2715504
HIV-1 p24 core antigen (clone MAK183, CM-IgG)	ExBIO	Cat# 11-CM006-BULK
Rabbit anti-p24 antiserum obtained by immunization of rabbits	Eurogentec	N/A
Peroxidase-AffiniPure goat anti-rabbit IgG, Fc fragment specific antibody	Dianova	Cat# 111-035-008; RRID: AB_2337937
IRDye® 680RD Goat anti-Mouse IgG (H + L)	LI-COR	Cat# 926-68070; RRID:AB_10956588
IRDye® 680RD Goat anti-Rabbit IgG (H + L)	LI-COR	Cat# 926-68071; RRID:AB_10956166
IRDye® 680RD Donkey anti-Goat IgG (H + L)	LI-COR	Cat# 926-68074; RRID:AB_10956736
IRDye® 800CW Goat anti-Mouse IgG (H + L)	LI-COR	Cat# 926-32210; RRID:AB_621842
IRDye® 800CW Goat anti-Rabbit IgG (H + L)	LI-COR	Cat# 926-32211; RRID:AB_621843
IRDye® 800CW Donkey anti-Goat IgG (H + L)	LI-COR	Cat# 926-32214; RRID:AB_621846
Donkey polyclonal anti-goat IgG (H+L), Alexa Fluor 647	Thermo Fisher	Cat# A-21447; RRID:AB_2535864
Donkey polyclonal anti-sheep IgG (H+L), Alexa Fluor 568	Thermo Fisher	Cat# A-21099; RRID:AB_2535753
Goat anti-mouse IgG (H + L), HRP	Thermo Fisher	Cat# A16066; RRID: AB_2534739
Goat anti-mouse IgG (H + L) Alexa Fluor 488	Thermo Fisher	Cat# A11001; RRID: AB_2534069
Bacterial and Virus Strains		
Escherichia coli XL-2 blue	Stratagene	Cat#200150
XL2-Blue MRF' TM Ultracompetent cells	Agilent Technologies	Cat#200151
Influenza A virus (H7N7), A/seal/Mass/1-SC35M/1980, GFP	M. Schwemmle (Reuther et al., 2015)	N/A
Measles virus, Schwarz-ATU-eGFP	This paper	N/A
ZIKV-MR766	J. Schmidt-Chanasit	N/A
Biological Samples		
Human: peripheral blood mononuclear cells (PBMCs)	DRK-Blutspendedienst Baden-Württemberg-Hessen, Ulm, Germany	N/A

(*Continued on next page*)

Continued

REAGENT or RESOURCE	SOURCE	IDENTIFIER
Human: lymphoid aggregate cultures (HLACs)	Bundeswehr Hospital Ulm, Germany	N/A
Chemicals, Peptides, and Recombinant Proteins		
L-Glutamine	Pan Biotech	Cat# P04-80100
Penicillin-Streptomycin	Thermo Fisher	Cat# 15140122
Fungizone	Thermo Fisher	Cat# 15290026
Non-Essential Amino Acids Solution	Thermo Fisher	Cat# 11140050
Sodium Pyruvate	Thermo Fisher	Cat# 11360070
Gentamicine Sulfate	Fisher Scientific	Cat# 30-005-CR
Timentin	GlaxoSmithKline	Cat# NDC 0029-6571-26 GSK
Human Serum	Sigma-Aldrich	Cat# H4522-100ML
Human M-CSF	R&D Systems	Cat# 216-MC-01M
Human IL-2 IS, premium grade	MACS Miltenyi Biotec	Cat#130-097-745
Remel PHA purified	Thermo Fisher	Cat# R30852801
Human Interferon α 2a	pbl assay science	Cat# 11101-1
IFNα subtypes	This paper	N/A
Human Interferon γ	Sigma-Aldrich	Cat# I3265
Dynabeads Human T-Activator CD3/CD28	Thermo Fisher	Cat# 111.32D
Biocoll Separation Solution	Biochrom	Cat# L6115
Lipofectamine RNAiMAX Transfection Reagent	Thermo Fisher	Cat# 13778150
TransIT LT-1	Mirus Bio	Cat# MIR2305
4X Protein Sample Loading Buffer	LI-COR	Cat# 928-40004
2-Mercaptoethanol	Sigma-Aldrich	Cat# M6250-100ML
BlueStar Plus Prestained Protein Marker	Nippon genetics	Cat# MWP04
NuPAGE 4-12% Bis-Tris Protein Gels	Invitrogen	Cat# NP0323BOX
		Cat# WG1403BOX
PVDF membrane	Merck Milipore	Cat# IPFL00010
Hoechst 33342 Solution	Thermo Fisher	Cat# #62249
Phalloidin Atto-647N	ATTO-TEC	Cat# AD647N-81
Fixable Viability Dye eFluor 780	Thermo Fisher	Cat# 65-0865-14
NucRed Live 647 ReadyProbes Reagent	Thermo Fisher	Cat# R37106
Pyr-RTKR-AMC	Bachem	Cat# I-1650
HIV-1 p24 protein (ELISA standard)	Abcam	Cat# 43037
KPL SureBlue TMB Microwell Peroxidase Substrate	Medac	Cat# 52-00-04
Trypsin from bovine pancreas, TPCK treated	Sigma-Aldrich	Cat# T1426
Avicel RC 581	FMC Biopolymers	Free sample
Pierce Protein A/G Magnetic Beads	Thermo Fisher	Cat# 88802
2-(4-Methylumbelliferyl)- α-D-N- acetylneuraminic acid sodium salt (MUNANA substrate)	GOLDBIO	Cat# M-520-25
Critical Commercial Assays		
GalScreen	Applied Biosystems	Cat# T1027
RosetteSep Human $CD4^+$ T Cell Enrichment Cocktail	Stem Cell Technologies	Cat# 15062
Luciferase Assay System	Promega	Cat# E1501
FIX & PERM Kit	Nordic-MUbio	Cat# GAS-002-1
Pierce HA Tag IP/CoIP Kit	Thermo Fisher	Cat# 26180
Phusion high-fidelity PCR Kit	Thermo Fisher	Cat# F553S
DNA Ligation Kit Ver. 2.1	TaKaRa	Cat# 6022

(*Continued on next page*)

Continued

REAGENT or RESOURCE	SOURCE	IDENTIFIER
Experimental Models: Cell Lines		
Human: HEK293T cells	ATCC	Cat# CRL-3216; RRID: CVCL_0063
Human: TZM-bl cells	NIH	Cat# 8129; RRID: CVCL_B478
Monkey: Vero E6 cells	ATCC	Cat# CRL-1586
Canine: MDCK cells	ATCC	RRID:CVCL_0422
Human: THP-1 cells	ATCC	Cat# TIB-202
Oligonucleotides		
Primers used to generate pCG IRES BFP expression plasmids	See table S1 of this paper	N/A
Primers used to generate pCAGGS expression plasmids	See table S2 of this paper	N/A
Primers used to generate chimeric HIV-1 proviral constructs	See table S3 of this paper	N/A
Primers used to generate measles virus clone	See table S4 of this paper	N/A
siRNA targeting GBP2 #1 (GCAGAAUUCCAAAGC AUCAdTdT)	Eurofins MWG	N/A
siRNA targeting GBP2 #2 (GGAUGUGGCUGAUG CACUUdTdT)	Eurofins MWG	N/A
siRNA targeting GBP5	Dharmacon	Cat# L-018178-01
Non-targeting control siRNA (UUCUCCGAACGUG UCACGUdTdT)	Eurofins MWG	N/A
Recombinant DNA		
Plasmid: pCG_hum GBP1 N-HA IRES BFP	Krapp et al., 2016	N/A
Plasmid: pCG_hum GBP2 N-HA IRES BFP	This paper	N/A
Plasmid: pCG_hum GBP3 N-HA IRES BFP	This paper	N/A
Plasmid: pCG_hum GBP4 N-HA IRES BFP	This paper	N/A
Plasmid: pCG_hum GBP5 N-HA IRES BFP	Krapp et al., 2016	N/A
Plasmid: pCG_hum GBP6 N-HA IRES BFP	This paper	N/A
Plasmid: pCG_hum GBP2 C588A N-HA IRES BFP	This paper	N/A
Plasmid: pCG_hum GBP5 C583A N-HA IRES BFP	Krapp et al., 2016	N/A
Plasmid: pCG_human furin C-AU-1 IRES BFP	This paper	N/A
Plasmid: pBR_HIV-1 M NL4-3	National Institute of Health (NIH)	Cat# 114
Plasmid: pBR_HIV-1 M NL4-3 Δ1Δ2	Münch et al., 2005	N/A
Plasmid: pBR_HIV-1 M NL4-3 Δ1Δ2 *nef*-	Münch et al., 2005	N/A
Plasmid: pBR_HIV-1 M NL4-3 Δ1Δ2 *nef*- (GBP5)	This paper	N/A
Plasmid: pBR_HIV-1 M NL4-3 Δ1Δ2 *nef*- (GBP5 C583A)	This paper	N/A
Plasmid: pBR_HIV-1 M NL4-3 Δ1Δ2 *nef*- (siRNA resistant GBP2)	This paper	N/A
Plasmid: pBR_HIV-1 M NL4-3 Δ1Δ2 *nef*- (siRNA resistant GBP5)	This paper	N/A
Plasmid: pCR-XL-TOPO_HIV-1 M subtype B CH058.c (transmitted founder virus)	B. Hahn (Ochsenbauer et al., 2012)	N/A
Plasmid: pCR-XL TOPO_HIV-1 M subtype C CH042 (transmitted founder virus)	B. Hahn (Freel et al., 2012)	N/A
Plasmid: pCR-XL-TOPO HIV-1 M subtype B CH077.t (transmitted founder virus)	B. Hahn (Ochsenbauer et al., 2012)	N/A
Plasmid: pCR-XL-TOPO_HIV-1 M subtype C CH164 (transmitted founder virus)	B. Hahn (Parrish et al., 2013)	N/A
Plasmid: pCR-XL TOPO_HIV-1 M subtype C CH185 (transmitted founder virus)	B. Hahn (Parrish et al., 2013)	N/A
Plasmid: pBR322HIV-1 M subtype C CH264 (transmitted founder virus)	B. Hahn (Salazar-Gonzalez et al., 2009)	N/A

(*Continued on next page*)

Continued

REAGENT or RESOURCE	SOURCE	IDENTIFIER
Plasmid: pBR332_HIV-1 M subtype B CH470 (transmitted founder virus)	B. Hahn (Parrish et al., 2013)	N/A
Plasmid: pBR332_HIV-1 M subtype C CH850 (transmitted founder virus)	B. Hahn (Fenton-May et al., 2013)	N/A
Plasmid: pHIV-1 AD8	V. Planelles (Zimmerman et al., 2006)	N/A
Plasmid: pCG_eGFP-GBP1 fusion protein	This paper	N/A
Plasmid: pCG_eGFP-GBP2 fusion protein	This paper	N/A
Plasmid: pCG_eGFP-GBP3 fusion protein	This paper	N/A
Plasmid: pCG_eGFP-GBP4 fusion protein	This paper	N/A
Plasmid: pCG_eGFP-GBP5 fusion protein	This paper	N/A
Plasmid: pCG_eGFP-GBP6 fusion protein	This paper	N/A
Plasmid: pCG_eGFP-GBP2 C588A fusion protein	This paper	N/A
Plasmid: pCG_eGFP-GBP5 C583A fusion protein	This paper	N/A
Plasmid: pCAGGS_HIV-1 M NL4-3 Env (137 FLAG-tag)	This paper	N/A
Plasmid: pCAGGS_HIV-1 M NL4-3 Env (137 FLAG-tag) ΔCT	This paper	N/A
Plasmid: pCAGGS_HIV-1 M NL4-3 Env (137 FLAG-tag) ΔCT/CD3ζ-TMD	This paper	N/A
Plasmid: pREP4_GPC3-HA	C. Goffinet (Veugelers et al., 2000)	N/A
Plasmid: pCR3.1_proMT1-MMP-HA	C. Goffinet (Coppola et al., 2008)	N/A
Plasmid: pBR_HIV-1 NL4-3.R*E*-F-Luc	Connor et al., 1995	N/A
Plasmid: pBR_HIV-1 NL4-3 *env* stop IRES eGFP	Wildum et al., 2006	N/A
Plasmid: pHIT-G_VSV-G (vesicular stomatitis virus glycoprotein)	Fouchier et al., 1997	N/A
Plasmid: pLTR-PV (Rabies virus strain PV glycoprotein)	Federici et al., 2009	N/A
Plasmid: pLTR_EBLV1 (European bat Lyssavirus 1 strain EBL1FRA glycoprotein)	Federici et al., 2009	N/A
Plasmid: pCAGGS_MaV GP (Marburg virus glycoprotein)	S. Becker (Wenigenrath et al., 2010)	N/A
Plasmid: pCMV_LasV GP (Lassa virus strain Josiah glycoprotein)	Simmons et al., 2003	N/A
Plasmid: pHCMV-based M288_IAV HA (H5N1 Influenza A/Thailand/KAN-1/2004 hemagglutinin)	Schmier et al., 2015	N/A
Plasmid: pHCMV-based M288_IAV NA (H5N1 Influenza A/Thailand/KAN-1/2004 neuraminidase)	Schmier et al., 2015	N/A
Plasmid: pBeloZIKV-SPH2015	(R.G., A.-K. Mattes, L. Issmail, M.W., G.S., L. Steppe, J.A.M., S.P., T. Grunwald, J.M., unpublished data)	N/A
Plasmid: pHHRz-MVvac2(eGFP)	This paper	N/A
Plasmid: p_MLV-env (murine leukemia virus glycoprotein)		N/A
Software and Algorithms		
BD FACSDiva Version 8.0	BD Biosciences	RRID: SCR_001456
Corel DRAW 2017	Corel Corporation	https://www.coreldraw.com/en/
GraphPad Prism Version 7.05	GraphPad Software, Inc.	https://www.graphpad.com; RRID: SCR_002798
LI-COR Image Studio Lite Version 3.1	LI-COR	https://www.licor.com/; RRID: SCR_013715
FlowJo_V10	FlowJo, LLC	https://www.flowjo.com; RRID:SCR_008520
ImageJ	Open source	https://imagej.nih.gov/ij/

(*Continued on next page*)

Continued

REAGENT or RESOURCE	SOURCE	IDENTIFIER
ZEN 2009	Carl Zeiss	https://www.zeiss.com/; RRID:SCR_013672
Multiple sequence alignment with hierarchical clustering	Corpet et al., 1999	http://multalin.toulouse.inra.fr
DNA/amino acid program Expasy-tool	SIB Swiss Institute of Bioinformatics	https://www.expasy.org/; RRID: SCR_012880
Other		
Expression profile of *GBP1*	Uhlén et al., 2015	https://www.proteinatlas.org/ENSG00000117228-GBP1/tissue
Expression profile of *GBP2*	Uhlén et al., 2015	https://www.proteinatlas.org/ENSG00000162645-GBP2/tissue
Expression profile of *GBP3*	Uhlén et al., 2015	https://www.proteinatlas.org/ENSG00000117226-GBP3/tissue
Expression profile of *GBP4*	Uhlén et al., 2015	https://www.proteinatlas.org/ENSG00000162654-GBP4/tissue
Expression profile of *GBP5*	Uhlén et al., 2015	https://www.proteinatlas.org/ENSG00000154451-GBP5/tissue
Expression profile of *GBP6*	Uhlén et al., 2015	https://www.proteinatlas.org/ENSG00000183347-GBP6/tissue
Expression profile of *GBP7*	Uhlén et al., 2015	https://www.proteinatlas.org/search/GBP7

CONTACT FOR REAGENT AND RESOURCE SHARING

Further information and requests for resources and reagents should be directed to and will be fulfilled by the Lead Contact, Daniel Sauter (daniel.sauter@uni-ulm.de).

EXPERIMENTAL MODEL AND SUBJECT DETAILS

Cell lines

HEK293T and TZM-bl cells were maintained in Dulbecco's modified Eagle medium (DMEM) supplemented with FCS (10%), L-glutamine (2 mM), streptomycin (100 μg/mL) and penicillin (100 U/mL) and were cultured at 37°C, 90% humidity and 5% CO_2. HEK293T cells were provided and authenticated by the ATCC. They were isolated from a female fetus and first described by DuBridge et al. (1987). TZM-bl cells were provided and authenticated by the NIH AIDS Reagent Program, Division of AIDS, NIAID, NIH from Dr. John C. Kappes, Dr. Xiaoyun Wu and Tranzyme Inc (Platt et al., 1998). TZM-bl cells are derived from HeLa cells, which were isolated from a 30-year-old female. Vero E6 (*Cercopithecus aethiops* derived epithelial kidney) cells used for ZIKV experiments, measles virus production and titer determination, were grown in Dulbecco's modified Eagle's medium (DMEM) supplemented with FCS (2.5%), L-glutamine (2 mM), streptomycin (100 μg/mL), penicillin (100 U/mL), sodium pyruvate (1 mM) and NEAA (1x). MDCK cells used for influenza virus production and titer determination were grown in Dulbecco's modified Eagle's medium (DMEM) supplemented with FCS (10%), L-glutamine (2 mM), streptomycin (100 μg/mL) and penicillin (100 U/mL). THP-1 cells were provided and authenticated by the ATCC and maintained in RPMI-1640 medium supplemented with FCS (10%), L-glutamine (2 mM), streptomycin (100 μg/mL) and penicillin (100 U/mL). THP-1 cells are monocyte-like cells, which adopt a macrophage-like phenotype upon PMA differentiation and were originally isolated from the peripheral blood of a 1-year-old male with acute monocytic leukemia. GBP5 knockout cell lines were created using CRISPR-Cas9 technology.

Primary cell cultures

PBMCs from healthy human donors were isolated using lymphocyte separation medium. $CD4^+$ T cells were negatively isolated using the RosetteSep Human $CD4^+$ T Cell Enrichment Cocktail according to the manufacturer's instructions. The purity of isolated $CD4^+$ T cells was analyzed by flow cytometry using anti-CD4 Per-CP and anti-CD11 FITC-conjugated antibodies. Purity was assumed sufficient when 90% of the cells were CD4-positive and CD11-negative. $CD4^+$ T cells were cultured in RPMI-1640 medium supplemented with FCS (10%), glutamine (2 mM), streptomycin (100 μg/mL), penicillin (100 U/mL) and interleukin-2 (IL-2) (10 ng/mL) at 37°C, 90% humidity and 5% CO_2.

Monocyte-derived macrophages (MDMs) were obtained by stimulation of PBMCs with recombinant human M-CSF (15 ng/mL) and human AB serum (10%) in DMEM supplemented with glutamine (2 mM), streptomycin (100 μg/mL) and penicillin (100 U/mL) for 7 days.

HLACs were obtained from tonsillar explants by hashing the tonsillar tissue. Cells were taken up and cultivated in RPMI-1640 medium supplemented with FCS (15%), glutamine (2 mM), streptomycin (100 μg/mL), penicillin (100 U/mL), fungizone (2.5 μg/mL), NEAA (1 x), MEM sodium pyruvate (1 mM), gentamicine sulfate (50 μg/mL) and timentin (310 μg/mL, freshly added) at 37°C, 90% humidity and 5% CO_2.

The use of human cells from peripheral blood and tonsillar explants was approved by the Ethics Committee of the Ulm University Medical Center (proposals #50/16 and #131/16, respectively). All donors provided informed written consent. Due to donor anonymization, the gender remained unknown.

METHOD DETAILS

Generation of GBP/furin expression plasmids

Expression plasmids for GBPs and furin were generated by gene amplification via PCR using human cDNA as template. Cloning into a pCG expression vector co-expressing BFP via an IRES was performed using unique XbaI and MluI restriction sites. Mutations disrupting the isoprenylation sites of GBP2 and GBP5 were introduced by the reverse PCR primers. eGFP-GBP fusion proteins were generated by fusing eGFP, a 3x(GGGGS) linker and the respective GBP sequence using overlap-extension PCR. To facilitate detection of the expressed proteins an N-terminal HA-tag (TACCCATACGATGTTCCAGATTACGCT) was introduced via the forward PCR primer in case of GBPs and a C-terminal AU1-tag (GACACCTACAGGTACATC) was introduced via the reverse PCR primer in case of furin. All constructs were sequenced to verify their integrity. PCR primers are listed in Table S1.

Generation of Env expression plasmids

The NL4-3 *env* ORF was amplified from proviral DNA and overlap-extension PCR was used to introduce a FLAG-tag (GATTACAAG GATGACGACGATAAG) after amino acid 136. Insertions at this position have previously been shown to be tolerated, with little effects on infectivity (Munro et al., 2014). The obtained DNA was cloned into a pCAGGS expression vector via unique EcoRI and KpnI restriction sites. This construct was used as PCR template for the generation of the NL4-3 FLAG-tagged ΔCT Env expression plasmid. The NL4-3 FLAG-tagged ΔCT/CD3ζ-TMD Env expression plasmid was generated by gene amplification via overlap-extension PCR from either an NL4-3 FLAG-tagged Env or a CD3ζ expression plasmid as template. All constructs were sequenced to verify their integrity. PCR primers are listed in Table S2.

Generation of HIV-1 chimeras expressing GBP2/5

To generate HIV-1 NL4-3 proviral plasmids encoding *GBP2/5* instead of *nef*, a previously described HIV-1 NL4-3 variant (named Δ1Δ2) was used, in which the *nef*/LTR overlap was removed and a unique MluI restriction site was inserted downstream of the *nef* stop codon (Münch et al., 2005). Overlap-extension PCR was used to generate siRNA resistant *GBP2/5* and to fuse the 3′ end of NL4-3 *env* carrying a HpaI restriction site with *GBP2/5* carrying a MluI restriction site at the 3′ end. The resulting DNA fragment was subsequently cloned into the HIV-1 NL4-3 proviral backbone via the HpaI and MluI restriction sites. All constructs were sequenced to verify their integrity. PCR primers are listed in Table S3.

Transfections and generation of virus stocks

HEK293T cells were transiently transfected using the calcium-phosphate precipitation method. One day before transfection, $6x10^5$ HEK293T cells were seeded in 6-well plates in 2 mL supplemented DMEM to obtain a confluence of 50%–60% at the time of transfection. For transfection, DNA was mixed with 13 μL 2 M $CaCl_2$ and filled up with water to 100 μL. Afterward, 100 μL 2 x HBS was added dropwise to this mixture, which was mixed by pipetting and added dropwise to the cells. To generate virus stocks, cells were transfected with proviral plasmids (5 μg). To test the antiviral effect of different GBPs, pCG-based expression constructs were co-transfected with proviral constructs. Whenever different amounts of pCG expression vectors were used within an experiment, empty vector control plasmids were used to keep the total DNA amount constant. The transfected cells were incubated for 16 h before the medium was replaced by fresh supplemented DMEM. Two days post transfection, cell culture supernatants were harvested and cleared by centrifugation at 660 x g for 3 min. To investigate the effects of GBP2/5 on ZIKV infectivity, HEK293T cells were co-transfected with pCG-based GBP expression constructs and a proviral plasmid containing the ZIKV-SPH2015 genome (R.G., A.-K. Mattes, L. Issmail, M.W., G.S., L. Steppe, J.A.M., S.P., T. Grunwald, J.M., unpublished data; Coffey et al., 2017; Cunha et al., 2016). Transfection was performed with TransIT LT-1 used at a reagent:DNA ratio of 3:1 according to the manufacturer's instructions. The transfected cells were incubated for 16 h before the medium was replaced by fresh supplemented DMEM additionally containing 25 mM HEPES. Two days post transfection, supernatants were harvested and cleared by centrifugation at 800 x g for 5 min.

Generation of a measles virus GFP reporter virus

To generate a modified measles virus cDNA clone with improved rescue efficiency, the measles virus cDNA was transferred from pB(+)MVvac2 (del Valle et al., 2007) into the backbone of pSAD-HH-L16-sc1 (Ghanem et al., 2012). The 5′ and 3′ parts of the measles virus antigenome sequence (nt 1-2045 and nt 9265-15984) were amplified separately by PCR. Both fragments were cloned into the backbone replacing the remaining L16 sequence. Finally, the remaining measles virus sequence (nt 2046-9264) was transferred into

the backbone, yielding pHHRz-MVvac2. An additional transcription unit (ATU) between the P and M genes was introduced via SalI as a 177 nt sequence (CCACCTAGTACAACCTAAATCCATTATAAAAAACTTAGGAACCAGGTCCACACAGCCGCCAGCCCATCAAC CATCCACTCCCACGATTGGAGCCATTCGAAGGCCGGCCGTACGTAGAGCGCTCGCGACGTCAGCGGCCGCCTACAGCTCAACTT ACCTGCCAACCCCATGCC) generating pHHRz-MVvac2-(ATU). Finally, to obtain pHHRz-MVvac2(eGFP), eGFP was cloned into ATU-MCS using the SnaBI/NotI sites. The recombinant virus was rescued as previously described (Radecke et al., 1995; Runge et al., 2014). PCR primers are listed in Table S4.

Generation of measles and influenza virus stocks

To generate measles virus stocks, Vero E6 cells were resuspended in a measles virus rescue stock and incubated for 1 h at 37°C. Every 15 min, cells were resuspended. After incubation, cells were resuspended in fresh supplemented DMEM and incubated at 37°C for up to 5 days until all cells were infected. Supernatants were discarded, infected cells were resupsended in fresh OPTI-MEM and viruses were released by one freeze/thaw cycle. Virus containing supernatants were cleared from cell debris by centrifugation, aliquoted and stored at −80°C.

To generate influenza virus stocks, MDCK cells were inoculated with influenza virus (MOI 0.01) containing 1 x MEM/BSA (for 2 x MEM/BSA: 20% MEM, 4 mM Glutamine, 200 μg/mL Streptomycin, 200 U/mL Penicillin, 0.42% BSA, 20 mM HEPES at pH 7.4, 0.24% $NaHCO_3$) supplemented with TPCK trypsin (1 μg/mL). After three days, supernatants were cleared from cell debris by centrifugation, aliquoted and stored at −80°C.

Titer determination of measles and influenza virus stocks

To determine the titer of GFP-expressing measles virus stocks, Vero E6 cells were seeded in 96-well plates and incubated for 3 h at 37°C. measles virus stocks were serially diluted from 1:10 to 1:1000000. Vero E6 cells were infected with 100 μL of the undiluted and diluted virus stocks. 48 h post infection, cells were washed with PBS, fixed with 4% PFA and virus foci (GFP positive foci) were counted under the microscope.

To determine the titer of influenza virus stocks, MDCK cells were seeded in 12-well plates one day prior to infection. Cell culture supernatants were removed, cells were washed with PBS and 100 μL of the undiluted and serially diluted influenza virus stocks from 1:10 to 1:1000000 were added with 250 μL 1 x MEM/BSA. Infected cells were incubated for 1 h at 37°C with regular shaking steps in between before 2 mL of overlay medium (50% 2 x MEM/BSA, 0.01% DEAE Dextran, 0.1% $NaHCO_3$, 0.6% Avicel RC 581, 1 μg/mL TPCK trypsin) was added to the cells. Three days post infection, supernatants were removed and cells were fixed with 4% PFA for 1 h at RT. Cells were washed with PBS and incubated in Crystal violet staining solution (0.5% Crystal violet, 30% Ethanol) for 10 min at RT. Cells were washed with H_2O and dried until plaques were counted under the microscope. The virus titer was calculated as plaque forming units per mL (PFU/mL).

Infection of TZM-bl reporter cells

To determine infectious HIV yield, 6,000 TZM-bl cells were seeded in 96-well plates, and infected with 5-100 μL cell culture supernatant in triplicates on the following day. Three days post infection, cells were lysed and *β-galactosidase* reporter gene expression was determined using the GalScreen Kit according to the manufacturer's instructions.

Stimulation of primary cells

MDMs were obtained by stimulation of PBMCs for 7 days with M-CSF and human serum (see "Primary cell cultures"). On day 7 of differentiation, MDMs were stimulated with IFNα2 (500 U/mL) or IFNγ (200 U/mL). Three days post stimulation, cells were harvested and lysed for analysis by western blotting.

$CD4^+$ T cells were stimulated with IL2 (10 ng/mL) + IFNα2 (500 U/mL), IL2 (10 ng/mL) + IFNγ (200 U/mL), IL2 (10 ng/mL) + anti-CD3/CD28 beads (cells:beads ratio 1:1), IL2 (10 ng/mL) alone or the different IFNα subtypes (50 ng/mL). Three days post stimulation, cells were harvested and lysed for analysis by western blotting.

Infection of primary cells

HLACs were infected with HIV-1 NL4-3 encoding *GBP5* instead of *nef* to determine the impact of GBP5 and the respective isoprenylation-deficient mutant on infectious virus release in primary HIV target cells. HEK293T cells were transfected with proviral constructs of HIV-1 NL4-3 encoding *GBP5* instead of *nef* or the respective control viruses (5 μg). Two days post transfection, supernatants were harvested and infectivity was adjusted using the TZM-bl reporter cell assay. HLACs were infected via spinoculation at 1200 x g for 2 h at 37°C. The input virus was washed away and infected HLACs were incubated for three days.

$CD4^+$ T cells were infected with HIV-1 NL4-3 or the indicated primary HIV-1 isolates to determine the impact of HIV-1 infection on GBP5 expression. $CD4^+$ T cells were primed with IL-2 (10 ng/mL) and PHA (1 μg/mL) for three days before infection via spinoculation at 1200 x g for 2 h at 37°C. The input virus was washed away and infected $CD4^+$ T cells were incubated for three days.

siRNA transfection and infection of macrophages

MDMs were obtained by stimulation of PBMCs for 7 days (see "Primary cell cultures"). On days 7 and 9 of differentiation, MDMs were transfected with GBP-specific siRNA pools or a non-targeting control siRNA. siRNA transfections were performed in 12-well plates

with two technical replicates for each sample using the Lipofectamine RNAiMAX transfection reagent. Before transfection, the medium was replaced by 500 μL fresh DMEM supplemented with FCS (10%), glutamine (2 mM), streptomycin (100 μg/mL) and penicillin (100 U/mL). For one well, 1.46 μL siRNA (20 μM) and 3 μL Lipofectamine RNAiMAX were mixed with 75 μL Opti-MEM, each. These two solutions were then mixed, incubated for 15 min at RT and added dropwise to the cells. 16 h after transfection on day 7 of differentiation, the medium containing the transfection mix was replaced by fresh DMEM supplemented with FCS (10%), glutamine (2 mM), streptomycin (100 μg/mL), penicillin (100 U/mL) and M-CSF (15 ng/mL). 8 h after transfection on day 9 of differentiation, cells were infected with AD8 or transduced with VSV-G pseudotyped HIV-1 NL4-3 encoding siRNA resistant *GBP* instead of *nef* or the respective control viruses. 12 h after infection, the input virus was removed by washing with 1 mL PBS and 1 mL fresh DMEM supplemented with FCS (10%), glutamine (2 mM), streptomycin (100 μg/mL) and penicillin (100 U/mL) was added to the cells. Infectious virus yield in cell culture supernatants was determined 6 days post infection by infection of TZM-bl reporter cells. To monitor knockdown efficiencies by western blotting, cells were harvested 6 days post infection, washed with 1 mL PBS and prepared according to the protocol "Western blotting."

Infection of THP-1 cells with measles, influenza A and Zika viruses

To determine the effect of GBP5 on measles and influenza virus replication, either THP-1 wild-type (WT) or GBP5 knockout (KO) cells were infected with GFP-expressing measles (strain Schwarz) or influenza (strain SC35M) virus. To this end, THP-1 cells were differentiated with PMA (100 nM) and, if indicated, stimulated with IFNγ (200 U/mL), each for 24 h. For infection with influenza viruses, cells were washed with PBS and virus was added in FCS free medium. For measles virus infection, virus was added in FCS containing medium. 6 h post infection, the input virus was removed by washing once with PBS and fresh medium (±FCS, ± IFNγ) was added to the cells. 24 h (influenza viruses) or 48 h (measles virus) post infection, virus replication was analyzed by quantifying neuraminidase activity in a MUNANA-assay (see "MUNANA assay") or by fluorescence imaging of GFP expression. For the latter, infected cells were washed with PBS and fixed with 4% PFA. Cell nuclei were stained with NucRed before GFP expression was analyzed with a Cytation3 imaging reader.

To determine the effect of GBP5 on Zika virus replication, either THP-1 WT or GBP5 KO cells were infected with Zika virus (strain MR766). To this end, THP-1 cells were differentiated with PMA (100 nM) for 24 h. Cells were infected with an MOI of 50. 12 h post infection, the input virus was removed by washing three times with PBS and fresh medium was added to the cells. Four days post infection, supernatants were harvested and used to infect Vero E6 cells to determine the $TCID_{50}$. To this end, 6,000 VeroE6 cells were seeded in 100 μL complete medium per well of a 96-well plate one day prior to infection. The next day, 80 μL medium were added, followed by 20 μL of 10-fold serially diluted supernatants in sextuplicates. 7 days post infection, the Zika virus induced cytopathic effect (CPE) was used to determine infected wells for $TCID_{50}$ calculation via Reed-Muench.

ELISA

To determine the amount of HIV-1 virions present in the supernatants of infected cells, the p24 capsid protein was quantified in a home-made p24 sandwich ELISA. High-binding ELISA plates (Sarstedt, #82.1581.200) were coated with the p24-coating antibody (ExBio, #11-CM006-BULK) overnight at RT. Plates were washed, blocked with PBS supplemented with 10% FCS for 2 h at 37°C and washed again before adding samples and p24 protein standard. After overnight incubation, plates were washed, incubated with a polyclonal anti-HIV p24 antiserum (home-made) and a secondary HRP-conjugated antibody (Dianova, #111-035-008), each for 1 h at 37°C. Plates were washed again, the TMB substrate was added and after several minutes of incubation the reaction was stopped with 0.5 M H_2SO_4. Absorption was measured at 450 nm with a baseline correction at 650 nm using a microplate reader.

Flow cytometry

Flow cytometry was used to determine GBP5 expression in HLACs and $CD4^+$ T cells after HIV-1 infection. Three days post infection, cells were harvested, washed in PBS with 1% FCS, fixed and permeabilized using the FIX&PERM kit according to the manufacturer's instructions. Cells were stained using goat anti-GBP5 (Santa Cruz, #sc-160353) and anti-goat AF647 (Thermo Fisher, #A-21447) as well as anti-p24 FITC (Beckman Coulter, #6604665) antibodies. Flow cytometric measurements were performed using a BD FACS Canto II flow cytometer. Mean fluorescence intensities (MFI) of GBP5 were determined in p24- and p24+ cells.

To determine Env cell surface expression levels in the presence of different GBPs, HEK293T cells were co-transfected with a proviral construct of NL4-3 *env* stop (2 μg), expression plasmids for the different GBPs (1.5 μg) and Env variants (0.1 μg). Two days post transfection, cells were harvested, washed in PBS with 1% FCS, stained using an anti-FLAG APC antibody (BioLegend, #637307) and fixed with 2% PFA for 30 min at 4°C before analysis with a BD FACS Canto II flow cytometer.

MUNANA assay

To determine neuraminidase activity in influenza virus (strain SC35M) infected THP-1 cells, a MUNANA (4-(methylumbelliferyl)-N-acetylneuraminic acid) assay was performed. 24 h post infection, cells were washed with PBS, lysed in 1% Triton X-100 and adequate sample dilutions were prepared in MES buffer (32.5 mM MES monohydrate, 4 mM $CaCl_2$ dihydrate). 20 μL sample was

incubated with 30 μL of MUNANA substrate (100 μM) and incubated for 4 h at 37°C. 150 μL stop solution (0.1 M glycine in 25% ethanol) was added to the reaction before neuraminidase activity was determined using a Cytation3 imaging reader (360 nm excitation and 450 nm emission).

Cell viability assay

To exclude toxicity of the GBP expression plasmids, a cell viability assay was performed. HEK293T cells were co-transfected with a proviral construct of HIV-1 CH058 (2.5 μg) and an expression plasmid for the different GBPs (2.5 μg) or a vector control (2.5 μg). Two days post transfection, cells were washed with PBS and incubated with a fixable viability stain (1 μL of EFluor™ 780 in 1 mL PBS for 1 million cells) for 15 min at RT. Cells were washed again and fixed with 2% PFA for 30 min at 4°C before analysis with a BD FACS Canto II flow cytometer.

Western blotting

To determine expression of cellular and viral proteins, cells were washed in PBS, lysed in western blot lysis buffer (150 mM NaCl, 50 mM HEPES, 5 mM EDTA, 0.1% NP40, 500 μM Na_3VO_4, 500 μM NaF, pH 7.5) and cleared by centrifugation at 20,800 x g for 20 min at 4°C. Lysates were mixed with Protein Sample Loading Buffer supplemented with 10% β-mercaptoethanol and heated at 95°C for 5 min. Proteins were separated on NuPAGE 4%–12% Bis-Tris Gels, blotted onto Immobilon-FL PVDF membranes and stained using primary antibodies directed against GBP2 (Santa Cruz, #sc-271568), GBP5 (Santa Cruz, #sc-160353), Furin (Abcam, #ab28547), HA-tag (Abcam, #ab18181), AU1-tag (Novus Biologicals, #NB600-453), V5-tag (Cell Signaling, #13202), HIV-1 Env (obtained through the NIH AIDS Reagent Program, Division of AIDS, NIAID, NIH: 16H3 mAb from Drs. Barton F. Haynes and Hua-Xin Liao) (Gao et al., 2009), Rauscher MLV gp70 (kindly provided by Christian Buchholz), p24 (Abcam, #ab9071), β-actin (Abcam, #ab8226), GAPDH (BioLegend, #631401), GFP (Abcam, #ab290) and Infrared Dye labeled secondary antibodies (LI-COR IRDye). Proteins were detected using a LI-COR Odyssey scanner and band intensities were quantified using LI-COR Image Studio Lite Version 3.1.

Co-immunoprecipitation

To investigate possible interactions between GBP2/5 or the respective isoprenylation-deficient mutants and furin, co-immunoprecipitation with subsequent analysis by western blotting was performed. HEK293T cells were co-transfected with expression plasmids for HA-tagged GBPs (1.5 μg) and AU1-tagged furin (1.5 μg). Two days post transfection, cells were lysed in 300 μL western blot lysis buffer and cleared by centrifugation (see "Western blotting"). 50 μL of the lysate was used for the whole-cell lysate analysis and further prepared as described in "Western blotting" while 250 μL of the lysate was used for the co-immunoprecipitation using the Pierce HA Tag IP/Co-IP Kit (Thermo Fisher) according to the manufacturer's instructions. Instead of the supplied loading dye, the LI-COR Protein Sample Loading Buffer was used. After co-immunoprecipitation, whole-cell lysates and precipitates were analyzed by western blotting.

To investigate possible interactions between endogenous GBP2/5 and furin, co-immunoprecipitation with subsequent analysis by western blotting was performed. MDMs were obtained by stimulation of PBMCs for 7 days with M-CSF and human serum (see "Primary cell cultures"). On day 7 of differentiation, MDMs were stimulated with IFNγ (200 U/mL). Three days post stimulation, cells were harvested, lysed in western blot lysis buffer, incubated on ice and cleared by centrifugation (see "Western blotting"). An aliquot was used for the whole-cell lysate control and further processed as described in "Western blotting." Furin was immunoprecipitated using anti-Furin antibodies (Abcam, #ab28547) and Pierce Protein A/G Magnetic Beads (Thermo Fisher). The respective isotype control (Abcam, #ab37415) was used to determine unspecific binding. Beads were washed three times with 1 mL NP40 wash buffer (50 mM HEPES, 300 mM NaCl, 0.5% NP40, pH 7.4) before incubation with 60 μL 1 x Protein Sample Loading Buffer (LI-COR) at 95°C for 10 minutes to recover bound proteins. After addition of 1.75 μL β-mercaptoethanol, whole-cell lysates and precipitates were analyzed by western blotting.

Microscopy

Confocal immunofluorescence microscopy was used to determine the subcellular localization of GBP1-6 and the isoprenylation-deficient mutants of GBP2 and GBP5. 75,000 HEK293T cells were seeded on 13 mm diameter glass coverslips coated with poly-L-lysine in 24-well plates. On the following day, cells were transfected with an expression plasmid for the different GBPs (250 ng). Two days post transfection, cells were fixed in 4% PFA for 20 min at RT, permeabilized in PBS 0.1% Triton X-100 for 5 min at RT and blocked in 1% BSA/PBS supplemented with 5% FCS for 30 min at RT. The nuclei, actin filaments and the trans-Golgi network were stained using Hoechst (Thermo Fisher, #62249), phalloidin Atto-647N (ATTO-TEC, #AD647N-81) and anti-TGN46 (Bio-Rad, #AHP500G) and anti-sheep AF568 (Thermo Fisher, #A-21099), respectively. Coverslips were mounted on glass slides using Mowiol mounting medium and confocal microscopy was performed using an LSM710 (Carl Zeiss).

4G2 immunostaining

Infectivity of the supernatants resulting from GBP-ZIKV co-transfection were determined by infection of Vero E6 cells. To this end, 6,000 Vero E6 cells were seeded in 100 μL complete medium per well of a 96-well plate and cultured overnight. The next day, 80 μL medium and 20 μL co-transfection supernatants were added in triplicates. Two days post infection, cells were washed with PBS and

fixed with 4% PFA for 20 min at RT. Cells were permeabilized with cold methanol for 5 min at 4°C, followed by washing with PBS. Next, cells were incubated with anti-flavivirus group antigen/protein E primary antibody (absolute antibody, #Ab00230-2.0) for 1 h at 37°C. Following three washing steps with PBS + 0.3% Tween, cells were incubated with an HRP-conjugated secondary antibody (Thermo Fisher, #A16066) and further incubated for 1 h at 37°C. Cells were finally washed four times before adding TMB peroxidase substrate. After 5 min incubation at RT, the reaction was stopped with 0.5 M H_2SO_4. Absorption was measured at 450 nm with a baseline correction at 650 nm using a VMax Kinetic ELISA microplate reader. For immunofluorescence microscopy of ZIKV infected cells, an AF488 coupled secondary antibody (Thermo Fisher, #A-11001) was used instead of the HRP-coupled antibody.

Furin activity assay

To determine furin activity in HEK293T cells, 22,000 cells were seeded in poly-L-lysine coated 96-well plates in 100 μL supplemented DMEM, one day before transfection. HEK293T cells were co-transfected in triplicates with different doses of expression plasmids for furin (0.5, 2.5, 12.5, 50 ng) and/or the different GBPs (75 ng). Two days post transfection, cell culture supernatants were harvested. Cells were washed with PBS, lysed with several freeze-thaw cycles and 100 μL H_2O per well was added. After 15 min incubation on ice, cell lysates were cleared by centrifugation. To determine the effect of endogenously expressed GBP5 on furin activity, THP-1 WT or GBP5 KO cells were seeded in 12-well plates (250,000 cells/well in 1 mL medium) and differentiated with PMA (100 nM). 24 h after seeding, fresh medium without PMA was added and, if indicated, cells were stimulated with IFNγ (200 U/mL) for 3 days, before cells were lysed in 1 mL H_2O by multiple freeze-thaw cycles. 20 μL of either cell culture supernatant or cell lysate were incubated with Pyr-Arg-Thr-Lys-Arg-7-Amido-4-methylcoumarin (AMC) substrate (1 nmol) and furin activity was determined for 60 min using a Cytation3 imaging reader (355 nm excitation and 460 nm emission).

Proteolytic processing of GPC3 and MMP14

To determine the effect of GBP2/5 on furin-mediated proteolytic processing of glypican-3 (GPC3) or matrix metalloproteinase-14 (MMP14), HEK293T cells were co-transfected with increasing amounts of an expression plasmid for the indicated GBPs (0, 0.5, 1.5, 2.5 μg), an expression plasmid for AU1-tagged furin (0.1 μg) and an expression plasmid for N-terminally HA-tagged GPC3 or C-terminally HA-tagged MMP14 (2.5 μg). Two days post transfection, cells were lysed and analyzed by western blotting. Band intensities were quantified and the ratios of cleaved products to total protein levels were calculated.

Firefly luciferase assay

For pseudotyping, an HIV-1 NL4-3 *env* stop firefly luciferase reporter plasmid (or an HIV-1 NL4-3 *env* stop IRES eGFP plasmid for western blot analysis) was used in combination with expression plasmids for the different viral glycoproteins (DNA amounts HIV-1 NL4-3 *env* stop/viral glycoprotein: EBLV-1, MLV, VSV: 2.4 μg/0.6 μg; MaV: 2.94 μg/0.06 μg; RabV, LasV: 1.8 μg/1.2 μg. In case of IAV, cells were transfected with equal amounts of plasmids expressing Hemagglutinin and Neuraminidase: 1.8 μg/0.6 μg/0.6 μg). Virus stocks were used to transduce HEK293T cells in triplicates, which were seeded one day prior to transduction in a 96-well plate format in a density of 10,000 cells/well. Three days post transduction, firefly luciferase activity was measured using Luciferase Cell Culture Lysis 5x Reagent and Luciferase Assay System according to the manufacturer's instructions.

QUANTIFICATION AND STATISTICAL ANALYSIS

Statistical analyses were performed using GraphPad PRISM 7. P values were calculated using paired or unpaired Student's t test or one sample t test. Unless otherwise stated, data are shown as mean of at least three independent experiments ± SEM. Significant differences are indicated as: * $p \leq 0.05$; ** $p \leq 0.01$; *** $p \leq 0.001$. Statistical parameters are specified in the figure legends.

ADDITIONAL RESOURCES

Tissue expression profile of human GBP1: https://www.proteinatlas.org/ENSG00000117228-GBP1/tissue;
Tissue expression profile of human GBP2: https://www.proteinatlas.org/ENSG00000162645-GBP2/tissue
Tissue expression profile of human GBP3: https://www.proteinatlas.org/ENSG00000117226-GBP3/tissue
Tissue expression profile of human GBP4: https://www.proteinatlas.org/ENSG00000162654-GBP4/tissue
Tissue expression profile of human GBP5: https://www.proteinatlas.org/ENSG00000154451-GBP5/tissue
Tissue expression profile of human GBP6: https://www.proteinatlas.org/ENSG00000183347-GBP6/tissue
Tissue expression profile of human GBP7: https://www.proteinatlas.org/ENSG00000213512-GBP7/tissue
Prediction of proprotein convertase target sequences: http://www.cbs.dtu.dk/services/ProP/